*Introduction of the EGFP gene*

Recombinant adenovirus carrying the enhanced green fluorescent protein (EGFP) gene was prepared as described [13]. Chorionic plate cells were plated on dishes at $2\times10^5/cm^2$, and infected with EGFP-expressing adenovirus at 10 plaque-forming units/cell on the next day. Chorionic plate cells were examined in vitro by fluorescent confocal microscopy for expression of the EGFP gene. By 7 days post-infection, nearly all of the cells expressed EGFP. To eliminate the possibility of free adenovirus in the cell supernatant, we infected murine fetal cardiomyocytes with chorionic plate cell supernatants after infection. No murine fetal cardiomyocytes expressed EGFP, implying that the cells are not transfected with free adenovirus.

*Preparation of murine fetal cardiomyocytes*

Fetal cardiomyocytes were obtained from the hearts of day 17 mouse fetuses. The hearts were minced with scissors and washed with PBS, and then incubated in PBS with 0.1% trypsin and 0.25 mM EDTA for 10 min at 37 °C. After DMEM supplemented with 10% FBS was added, the cardiomyocytes were centrifuged at 1000 rpm for 5 min. The pellet was then re-suspended in 10 ml of DMEM with 10% FBS and incubated on glass dishes for 1 h to separate the cardiomyocytes from fibroblasts. The floating cardiomyocytes were collected and re-plated at $5\times10^4/cm^2$.

*Co-culture system of chorionic plate cells and murine fetal cardiomyocytes*

Neither 5-azaC [12] nor oxytocin [21] was used in this process as they are known to initiate cardiomyogenic differentiation. EGFP-labeled chorionic plate cells were harvested with 0.25% trypsin and 1 mM EDTA and overlaid onto the cultured fetal cardiomyocytes at $7\times10^3/cm^2$. Every 2 days the culture medium was replaced with fresh culture medium that was supplemented with 10% FBS and 1 μg/ml Amphotericin B (Gibco). The morphology of the beating EGFP-labeled chorionic plate cells was evaluated under a fluorescent microscope. The image was monitored using a CCD camera and stored as digital video. The cell contraction was analyzed using an image-edge detection program made by Igor Pro 4 (Wavemetrics Inc., Lake Oswego, Oregon).

*Electrophysiological analysis*

On day 10 of co-cultivation, action potentials (APs) were recorded as described previously [12,13] from spontaneously beating EGFP-labeled cells. Spontaneously beating EGFP-positive chorionic plate cells were selected as targets. The APs of the targeted cells had been recorded and Alexa568 dye was injected by iontophoresis to confirm that the APs were generated by EGFP-positive chorionic plate cells. The extent of dye transfer was monitored under a fluorescence microscope, and digital images were recorded with a digital photo camera (D100; Nikon, Tokyo, Japan) mounted on a microscope with a fluorescence filter (UMWIG2; Olympus).

*Immunocytochemistry*

A laser confocal microscope (LSM510, Zeiss) was used for immunocytochemical analysis. The chorionic plate cells co-cultured with fetal cardiomyocytes in vitro were fixed with 2% paraformaldehyde (PFA) in PBS for 20 min at 4 °C and treated with 0.1% Triton-X PBS for 20 min at room temperature. These cells were then stained with mouse monoclonal anti-human cardiac troponin-I antibody (#4T21/19-C7 HyTest, Euro, Finland) diluted 1:300, monoclonal anti-α-actinin antibody (Sigma) diluted 1:300, and anti-connexin 43 antibody (Sigma) diluted 1:300. To prevent fading and to stain nuclei, a Slow Fade Light Antifade kit with 4′-6-diamidino-2-phenylindole (DAPI) (Molecular Probes) was used.

## Results

*Establishment of chorionic plate cells*

Almost all human tissues or organs can be a source of MSCs, which have been extracted from fat, muscle, menstrual blood, endometrium, placenta, umbilical cord, cord blood, skin, and eye. In this study, we focused on cells derived from fetuses, since fetus-derived cells tend to both differentiate and proliferate better than adult cells [22]. In that sense, human placenta is a good source of fetus-derived MSCs. We cultivated chorionic plate cells that were obtained from the chorionic mesoderm of the placenta (Fig. 1A). The chorionic plate cells regarded as being Population Doubling (PD) 0 or Day 0 were fibroblast-like in morphology, indistinguishable in appearance from the marrow-derived MSCs, and relatively larger in size than rapidly self-renewing stem cells [23] (Fig. 1B). The cells from PD 9 to PD 18 rapidly proliferated in culture and were propagated continuously. Chorionic plate cells did not undergo malignant transformation. They stopped dividing after reaching confluence and they did not form any foci after reaching confluence in vitro.

To clarify the character of the established chorionic plate cells, we first performed karyotypic analysis of 30 cells at PD 3. All cells had normal chromosomes without any chromosomal aberration (Fig. 1C). The sex chromosomes were found to be XY, implying that all cells were of fetal origin. Genomic FISH analysis also revealed that all cells had XY chromosomes (Fig. 1D). We examined the cell surface marker of the placenta-derived cells (chorionic plate cells) by FACS analysis (Fig. 1E). The surface markers of chorionic plate cells are exactly the same as those of previously reported bone-marrow- and cord blood-derived mesodermal cells, i.e., positive for CD29, CD44,

**Fig. 3 – Immunocytochemistry of chorionic plate cells for human cardiac troponin-I. (A–F) Immunocytochemistry of differentiated chorionic plate cells with anti-human cardiac troponin-I (cTnI) antibody. The EGFP-positive cells (B) were stained with anti-human cTnI antibody (A) and the merged image (DAPI, EGFP, cTnI) is shown in panels D and F. An enlarged image (red square in D) is shown in panel E. Clear striations were observed with red fluorescence of cTnI in the differentiated cells. (G–I) A merged image for EGFP and cTnI is shown in panel G. A longitudinal section at the green line in the merged image G is shown in panel H. An axial section at the red line in merged image G is shown in panel I.**

CD59, CD73, CD 90, CD105 and CD166, and negative for CD14, CD31, CD34 and CD45.

Next we investigated whether chorionic plate cells have cardiomyogenic potential by human cardiomyocyte-specific gene expression using RT-PCR method (Fig. 2, Table 1) and gene chip analysis (Table 2; GEO accession number, GSE7021: GSM162104 and GSM162105). Chorionic plate cells expressed Csx/Nkx-2.5, GATA4, BNP, cardiac troponin T (cTnT), cardiac

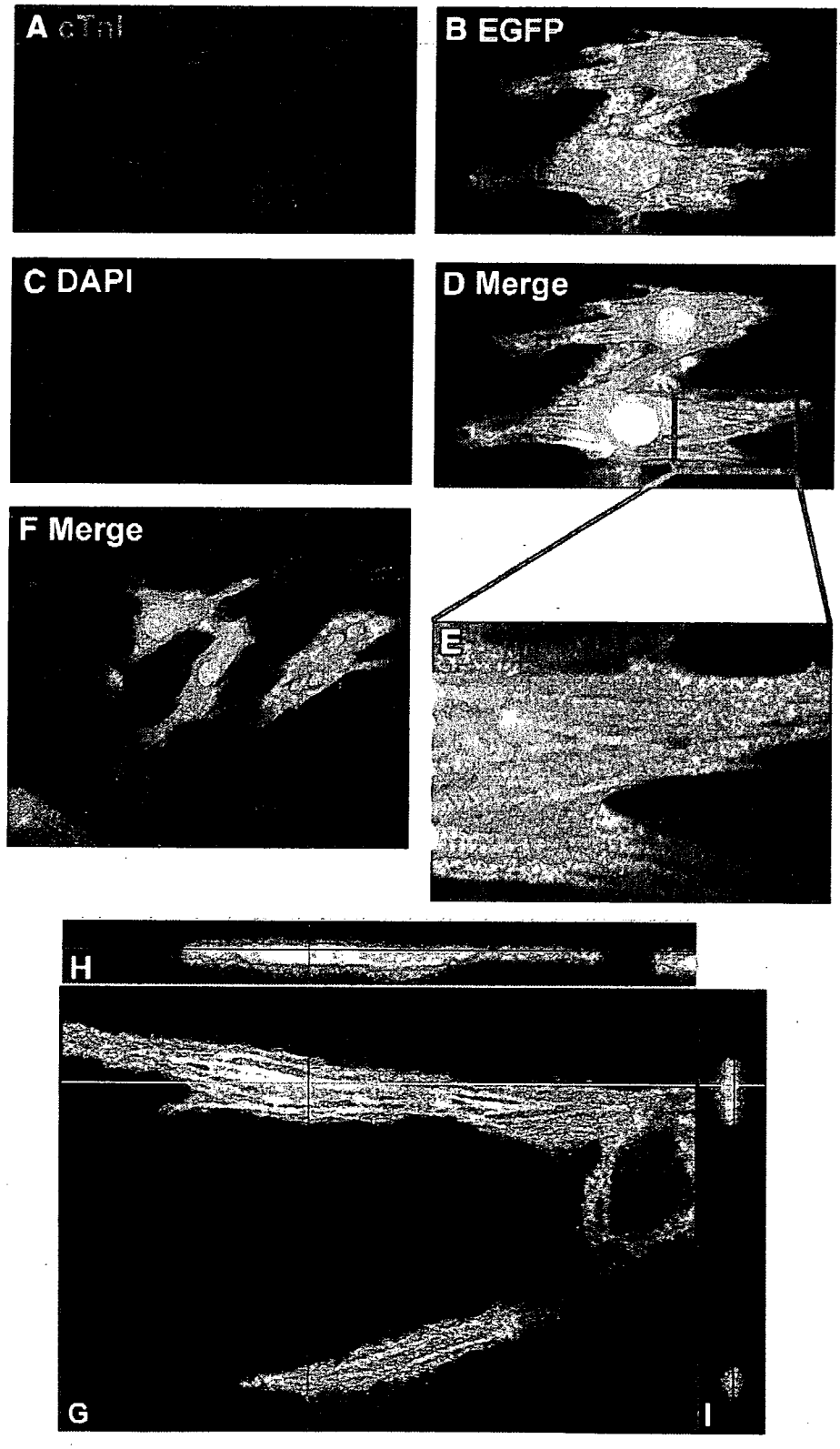

actin and myosin light chain-2α (MLC-2α) in the default state, implying that chorionic plate cells can differentiate into cardiomyocytes, like CMG cells in which Csx/Nkx-2.5 and GATA4 are constitutively expressed before induction [12].

### *Cardiomyogenic differentiation of chorionic plate cells*

employed a co-culture system with murine fetal cardiomyocytes to induce cardiac differentiation, since in vitro simulation of the heart by the environment has been shown to be an efficient means of inducing the differentiation of human endothelial progenitor cells [15] and human marrow stromal cells [13]. EGFP-labeled chorionic plate cells were co-cultured with murine fetal cardiomyocytes without any chemical treatment. A few EGFP-positive chorionic plate cells started to contract on day 3 after the start of co-cultivation, and beat strongly and rigorously in a synchronized manner on day 5 (Supplementary movie 1). The cells continued to beat at least until day 21 during the period of observation. The frequency of cardiomyogenic differentiation from chorionic plate cells was calculated based on the number of cTnI-positive cells. In three independent experiments, the percentage of cells that underwent cardiomyogenic differentiation was similar (15.1±5.1%) (Supplementary Fig. 1S). Our investigation of the cardiomyogenic-specific gene expression for differentiated chorionic plate cells (Fig. 2) found that cardiac actin was fully expressed, whereas Csx/Nkx-2.5 and cardiac troponin T were only slightly expressed. GATA4, cTnI, MLC-2α, and BNP were not expressed. Technical difficulties may have adversely affected these results, as some of the differentiated cells divided from murine fetal cardiomyocytes were physically damaged and so the ratio of differentiated to undifferentiated cells may well have been diminished in each case. In fact, in every experiment, cTnI was detected by immunocytochemical analysis. Immunocytochemical staining revealed that EGFP-labeled cells stained positive for cTnI (Figs. 3A–F). Immunostaining of longitudinal sagittal and axial transverse sections confirmed that cTnI was expressed in the EGFP-positive cells (Figs. 3G–I, Supplementary movie 2). These results imply that co-culture system of chorionic plate cells and murine embryonic cardiomyocytes induces differentiation of chorionic plate cells into cTnI-positive cells in vitro. cTnI-positive cells were evenly detected throughout the dish, suggesting that the cardiomyogenic induction rate was quite high in the present model. The EGFP-positive cells also expressed α-actinin, and connexin 43 (Figs. 4A–E). Clear striations were observed for the red fluorescence of cTnI (Fig. 3A) and α-actinin (Fig. 4A) in the differentiated chorionic plate cells. Connexin 43 staining (Figs. 4C–G) showed a clear and diffuse pattern around the margin of the cytoplasm, suggesting that these human transdifferentiated cardiomyocytes have tight electrical coupling with each other. We also performed in vivo implantation of EGFP-labeled chorionic plate donor cells into the ischemic heart model of nude rats (data not shown). EGFP-labeled chorionic plate donor cells exhibit positive cTnI reactivities at the implanted site. However, the frequency of cTnI-positive cells in vivo is not comparative with that in vitro.

To investigate if chorionic plate cells are capable of differentiating into osteoblasts and adipocytes [19,20], we induced chorionic to differentiate into osteocytes and adipocytes under specific culture conditions. Chorionic plate cells did not show clear adipogenic and osteogenic differentiation: cells did not accumulate Oil Red O-positive fat droplets and calcium, and did not increase alkaline phosphatase osteogenic activity (Supplementary Fig. 2S), suggesting that chorionic plate cells have a cardiomyocyte potential, but not adipocyte or osteoblast potential.

### *The action potential of differentiated chorionic plate cells*

To detect the electrophysiological coupling due to gap-junctional communication between beating cardiomyocytes, action potentials (APs) were recorded from spontaneously beating EGFP-positive cells. Alexa568 was injected into cells via a recording microelectrode to stain the cells and to confirm that the APs were generated by EGFP-positive cells (Figs. 5A–C). The dye did not diffuse into the murine cardiomyocytes, indicating that there were no tight cell-to-cell heterologous connections, i.e., gap junctions. Alexa568 dye did not diffuse into adjacent human and murine cells of the injected cells that exhibited action potentials. The action potentials obtained originate from human chorionic plate cells or may result from electrical coupling with adjacent cardiomyocytes [24]. The APs obtained from chorionic plate cells showed clear cardiomyocyte-specific sustained plateaux (Figs. 5D, E) and were therefore concluded to be APs of cardiomyocytes, not of smooth muscle cells, nerve cells, or skeletal muscle cells. The measured parameters of the recorded AP were averaged (Fig. 5F). Chorionic plate cells had the character of 'working' cardiomyocytes or ordinary cardiomyocytes. The rhythm of almost all the beating cells had become regular at 1 week. The fractional shortening (%FS) of the cells was analyzed (Supplementary Fig. 3S), using a cell-edge detection program developed by S.M. The EGFP-positive cells contracted simultaneously within the whole visual field, suggesting tight electrical communication among them. The average %FS was 5.46±0.40% ($n$=10). In summary, human cardiomyocytes obtained from the chorionic plate cells were electrophysiologically and physiologically functional.

## Discussion

### *Transdifferentiation of human extraembryonic mesodermal cells into embryonic mesodermal cells: functional working cardiomyocytes*

This study was conducted to determine whether extensive ex vivo propagation by cell culture would prevent the cardiomyogenic differentiation of placenta-derived cells. According to our previous study on the induction of cardiomyogenic differentiation of immortalized murine marrow stromal cells [12,15] and human marrow stromal cells [13] by demethylating agents, the transdifferentiation of human stromal cells was limited to working cardiomyocytes and did not include pacemaker cells. This was probably due to the origin of cells, that is, the default state of the chorionic plate-derived human fetal cells used in the experiment. The idea for the cardiomyogenic differentiation protocol using murine fetal cardiomyocytes without 5-azacytidine arose from reports that endothelial cells differentiate into cardiomyocytes as a result of co-cultivation with murine fetal cardiomyocytes [25].

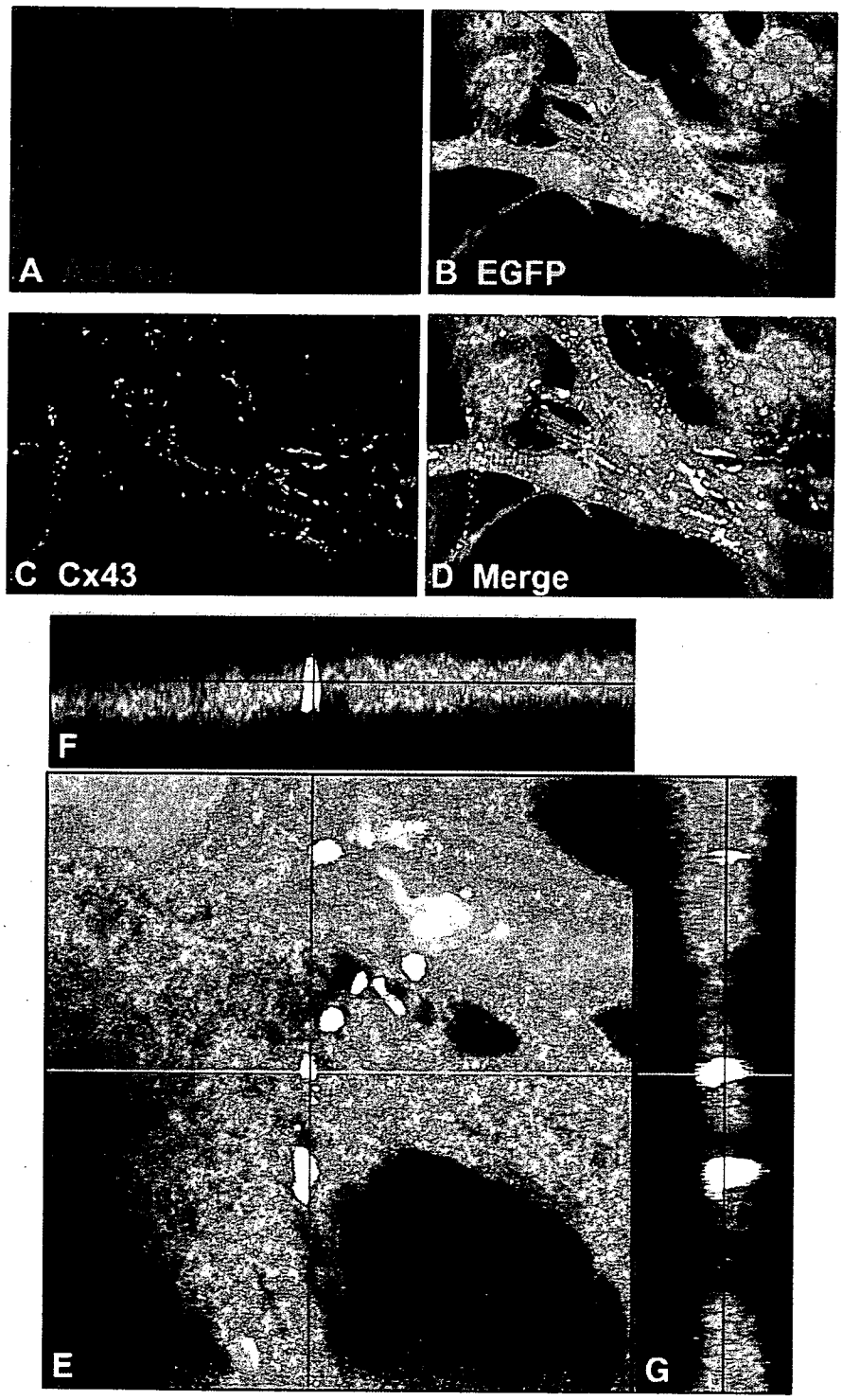


Fig. 4 – Immunocytochemistry of chorionic plate cells for α-actinin and connexin 43. (A–D) Immunocytochemistry of differentiated chorionic plate cells for α-actinin (Actinin) and connexin 43 (Cx43) antibody. Clear striations were observed for the red fluorescence of α-actinin (A) in the EGFP-positive cells (B). Connexin 43 (C) was stained along the attachment site of EGFP-positive cells. Merged images (α-actinin, connexin 43, EGFP) are shown in panel D. (E–G) A merged image for α-actinin, connexin 43, and EGFP is shown in panel E. (F) A longitudinal section at the green line in merged image E. (G) An axial section at the red line in merged image E. Panels F and G show that connexin 43 is located between EGFP-positive cells.

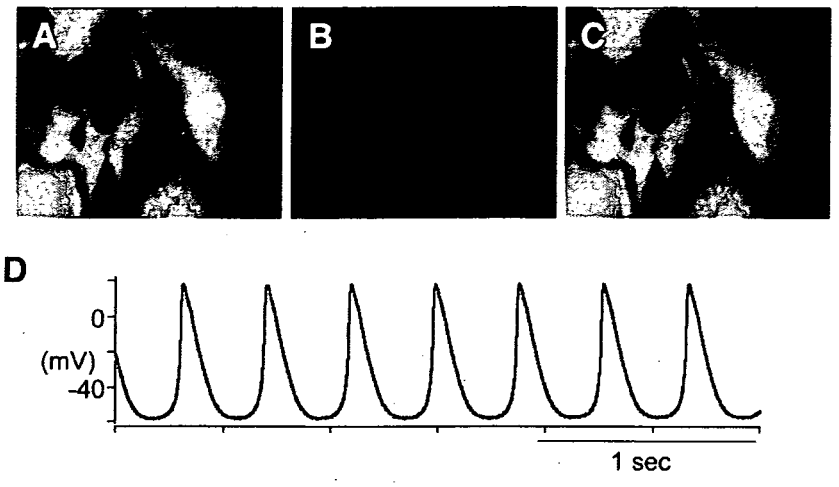


F

| | Amplitude (mV) | Resting Membrane Potential (mV) | APD90 (msec) | APD50 (msec) | RR (sec) | Vmax (V/s) | n |
|---|---|---|---|---|---|---|---|
| PLKC | 63.87± 2.24 | -52.22± 1.05 | 209.1± 12.9 | 100.2± 4.8 | 0.948± 0.138 | 4.460± 0.355 | 14 |

**Fig. 5 – Electrophysiological and physiological analysis of chorionic plate cells. (A–C) EGFP-labeled chorionic plate cells were injected with Alexa568 solution by ionophoresis through a microelectrode. (D, E) Two different types of action potential, i.e., tachycardia type and bradycardia type, were recorded. Both types of cells had the features of working cardiomyocytes. The rhythm of their beating was regular. (F) The measured action potential parameters of EGFP-labeled chorionic plate cells are averaged.**

The high frequency of cardiomyogenic differentiation makes it inconceivable that the transdifferentiation is due to fusion; in addition, bone marrow stromal cells [13] do not fuse with feeder cells in the co-cultivation system and the frequency of fusion in the co-culture system is not high [26] in contrast to myogenic differentiation [27]. The global gene expression pattern showed that the change in gene expression during differentiation was consistent with phenotypic alteration. The cells established from the placenta can be extensively and clonally expanded in vitro while retaining their potential to differentiate into cardiomyocytes that exhibit spontaneous beating and cardiomyocyte-specific action potential under in vitro conditions. This differentiation potential shown by the placenta-derived cells is the same as that reported for bone marrow MSCs [12,13,15]. It is also noteworthy that the transdifferentiation of chorionic plate cells represents the transition from extraembryonic cells to embryonic cells, while the transdifferentiation from bone-marrow-derived MSCs to neurogenic cells, which we previously reported [28,29], is transition between germ layers in embryonic tissues.

Most of the surface markers of the placenta-derived cells examined in this study are the same as those detected in their bone marrow counterparts [13,30], with both cord blood- and bone-marrow-derived mesodermal cells being positive for CD29, CD44, and CD59, and negative for CD34. Our finding of in vitro differentiation from extraembryonic mesodermal cells to embryonic mesodermal cells in this study, a key future goal for any cell-based therapy, could thus be achieved by exposing placenta-derived cells to murine fetal cardiomyocytes, at least in vitro. This technique allows the applications of the placenta to be further extended and permits it to be used as an alternative to bone marrow as a source of cells with cardiomyogenic potential.

### *Is the high rate of cardiomyogenic differentiation of placenta-derived cells due to the default cell state?*

The cardiomyogenic differentiation rate of chorionic plate cells (15.1%) was relatively high compared to that of marrow-derived MSCs (less than 0.3%) [13]. The gene expression

pattern of chorionic plate cells before cardiomyogenic differentiation was different from that of marrow-derived MSCs. The expression of cardiomyocyte-associated genes in the chorionic plate cells, which we unexpectedly found by GeneChip analysis and confirmed by RT-PCR, is surprising. Constitutive expression of the Csx/Nkx2.5 cardiogenic 'master' gene [31,32] in the chorionic plate cells with the ability of self-renewal suggests that the chorionic plate cells have cardiogenic potential [33] and may be termed "cardiac precursor cells" in the light of their biological characteristics like endometrium-derived myogenic procursor cells [27]. The mechanism of the drastic improvement in the differentiation rate of chorionic plate cells may be attributable to default characteristics as cardiac precursor cells of the placenta-derived cells in culture. Because of this improvement in the differentiation rate, it is possible to obtain a large number of cardiomyocytes without prolongation of their life span, i.e., transfer of oncogenic molecules into cells, to restore cardiac function. It is quite interesting that working cardiomyocytes can be generated from placenta-derived cells, since one of the types of target cells for regenerative medicine is heart cells.

### *Are human placenta-derived cells that are propagated in vitro useful for cell-based therapy?*

Can primary placenta-derived cell 'culture' contribute to cell-based therapy or regenerative medicine? Primary placenta-derived cell culture obtained from the chorionic mesodermal layer succeeded in almost 100% of the attempts, and the cells were passaged only 3 or 4 times (6 to 7 PDs) before reaching premature senescence. The problems involved in cell-based therapy with human placenta-derived cells are the finite life span of the cells and the difficulty of obtaining a large enough number of cells. Based on the results of our previous study using cord blood-derived cells, the establishment of cells can be explained by: (1), lack of $p16^{INK4a}$ in primary-cultured cells, or (2), selection of cells that do not express $p16^{INK4a}$ from a heterogeneous population [22]. We cannot exclude either possibility, and we did observe two different types of cells, i.e., rapidly growing spindle cells and quiescent flat and elongated cells in the primary culture of placenta cells. Experimental settings that allow human placenta cells to double more than 100 times may be used to obtain a large number of cells at least from the placenta.

We believe that these placenta-derived extraembryonic mesodermal cells may be used to supply cardiomyocytes to patients with ischemic heart disease, dilated cardiomyopathy, and Kawasaki disease, which all have a poor prognosis and are sometimes lethal. The 'risk versus benefit' balance is essential when applying these multiplied cells clinically and the 'risk' or 'drawback' in this case is the transformation of implanted cells. In vivo experiments revealed that no tumor was observed for up to 4 weeks when chorionic plate cells at P5 ($1\times10^7$) were subcutaneously inoculated into immunodeficient, non-obese diabetic (NOD)/severe combined immunodeficiency (SCID)/interleukin 2 $receptor^{-/-}$ (NOG) mice (data not shown). Human placenta-derived cells spontaneously avoid premature senescence without gene induction and enter replicative senescence. Replicative senescence may be due to a tumor suppressor mechanism that avoids the risk of cell transformation after implantation of cells as a source for cell-based therapy [34].

Our present study suggested the presence of a precursor cell type in the placenta which is destined to generate 'working cardiomyocytes'. Since the placenta is usually discarded, it can be collected at usual delivery or cesarean section and can be banked or stored. Cells with almost all the HLA types can be collected after several generations. A placenta-derived cell bank system covering all HLA types may be necessary for patients who cannot supply bone marrow cells but want to receive stem cell-based cardiac therapy.

## Acknowledgments

We would like to express our sincere thanks to A. Crump for critically reading the manuscript, A. Oka and M. Terai for the support throughout the work, and K. Saito for the secretarial work. This study was supported by grants from the Ministry of Education, Culture, Sports, Science and Technology (MEXT) of Japan; by the Suntory Fund for Advanced Cardiac Therapeutics, Keio University School of Medicine; Health and Labor Sciences Research Grants, and the Pharmaceuticals and Medical Devices Agency; by the Research on Health Science Focusing on Drug Innovation from the Japan Health Science Foundation; by the Program for Promotion of Fundamental Studies in Health Science of the Pharmaceuticals and Medical Devices Agency (PMDA); by a research Grant for Cardiovascular Disease from the Ministry of Health, Labor and Welfare; by a Grant for Child Health and Development from the Ministry of Health, Labor and Welfare; and by a grant from Terumo Life Science Foundation. A part of the work was done at the Pfizer Keio Research Laboratory Center for Integrated Medical Research.

Data set from the gene chip analysis are available at the GEO database with accession number GSE7021: GSM162104 and GSM162105.

## Appendix A. Supplementary data

Supplementary data associated with this article can be found, in the online version, at doi:10.1016/j.yexcr.2007.04.028.

## REFERENCES

[1] T. Thom, N. Haase, W. Rosamond, V.J. Howard, J. Rumsfeld, T. Manolio, Z.J. Zheng, K. Flegal, C. O'Donnell, S. Kittner, D. Lloyd-Jones, D.C. Goff Jr., Y. Hong, R. Adams, G. Friday, K. Furie, P. Gorelick, B. Kissela, J. Marler, J. Meigs, V. Roger, S. Sidney, P. Sorlie, J. Steinberger, S. Wasserthiel-Smoller, M. Wilson, P. Wolf, Heart disease and stroke statistics—2006 update: a report from the American Heart Association Statistics Committee and Stroke Statistics Subcommittee, Circulation 113 (2006) e85–e151.

[2] A. Leri, J. Kajstura, P. Anversa, Cardiac stem cells and mechanisms of myocardial regeneration, Physiol. Rev. 85 (2005) 1373–1416.

[3] M.A. Laflamme, C.E. Murry, Regenerating the heart, Nat. Biotechnol. 23 (2005) 845–856.

[4] H.F. Tse, Y.L. Kwong, J.K. Chan, G. Lo, C.L. Ho, C.P. Lau, Angiogenesis in ischaemic myocardium by intramyocardial autologous bone marrow mononuclear cell implantation, Lancet 361 (2003) 47–49.
[5] E. Perin, Transendocardial injection of autologous mononuclear bone marrow cells in end-stage ischemic heart failure patients: one-year follow-up, Int. J. Cardiol. 95 (Suppl 1) (2004) S45–S46.
[6] K.C. Wollert, G.P. Meyer, J. Lotz, S. Ringes-Lichtenberg, P. Lippolt, C. Breidenbach, S. Fichtner, T. Korte, B. Hornig, D. Messinger, L. Arseniev, B. Hertenstein, A. Ganser, H. Drexler, Intracoronary autologous bone-marrow cell transfer after myocardial infarction: the BOOST randomised controlled clinical trial, Lancet 364 (2004) 141–148.
[7] O. Agbulut, S. Vandervelde, N. Al Attar, J. Larghero, S. Ghostine, B. Leobon, E. Robidel, P. Borsani, M. Le Lorc'h, A. Bissery, C. Chomienne, P. Bruneval, J.P. Marolleau, J.T. Vilquin, A. Hagege, J.L. Samuel, P. Menasche, Comparison of human skeletal myoblasts and bone marrow-derived CD133+ progenitors for the repair of infarcted myocardium, J. Am. Coll. Cardiol. 44 (2004) 458–463.
[8] P. Menasche, A.A. Hagege, M. Scorsin, B. Pouzet, M. Desnos, D. Duboc, K. Schwartz, J.T. Vilquin, J.P. Marolleau, Myoblast transplantation for heart failure, Lancet 357 (2001) 279–280.
[9] D.J. Prockop, Stem cell research has only just begun, Science 293 (2001) 211–212.
[10] K. Le Blanc, C. Gotherstrom, O. Ringden, M. Hassan, R. McMahon, E. Horwitz, G. Anneren, O. Axelsson, J. Nunn, U. Ewald, S. Norden-Lindeberg, M. Jansson, A. Dalton, E. Astrom, M. Westgren, Fetal mesenchymal stem-cell engraftment in bone after in utero transplantation in a patient with severe osteogenesis imperfecta, Transplantation 79 (2005) 1607–1614.
[11] K. Le Blanc, I. Rasmusson, C. Gotherstrom, C. Seidel, B. Sundberg, M. Sundin, K. Rosendahl, C. Tammik, O. Ringden, Mesenchymal stem cells inhibit the expression of CD25 (interleukin-2 receptor) and CD38 on phytohaemagglutinin-activated lymphocytes, Scand. J. Immunol. 60 (2004) 307–315.
[12] S. Makino, K. Fukuda, S. Miyoshi, F. Konishi, H. Kodama, J. Pan, M. Sano, T. Takahashi, S. Hori, H. Abe, J. Hata, A. Umezawa, S. Ogawa, Cardiomyocytes can be generated from marrow stromal cells in vitro, J. Clin. Invest. 103 (1999) 697–705.
[13] Y. Takeda, T. Mori, H. Imabayashi, T. Kiyono, S. Gojo, S. Miyoshi, N. Hida, M. Ita, K. Segawa, S. Ogawa, M. Sakamoto, S. Nakamura, A. Umezawa, Can the life span of human marrow stromal cells be prolonged by bmi-1, E6, E7, and/or telomerase without affecting cardiomyogenic differentiation? J. Gene Med. 6 (2004) 833–845.
[14] D. Orlic, J. Kajstura, S. Chimenti, I. Jakoniuk, S.M. Anderson, B. Li, J. Pickel, R. McKay, B. Nadal-Ginard, D.M. Bodine, A. Leri, P. Anversa, Bone marrow cells regenerate infarcted myocardium, Nature 410 (2001) 701–705.
[15] S. Gojo, N. Gojo, Y. Takeda, T. Mori, H. Abe, S. Kyo, J. Hata, A. Umezawa, In vivo cardiovasculogenesis by direct injection of isolated adult mesenchymal stem cells, Exp. Cell Res. 288 (2003) 51–59.
[16] J.S. Wang, D. Shum-Tim, J. Galipeau, E. Chedrawy, N. Eliopoulos, R.C. Chiu, Marrow stromal cells for cellular cardiomyoplasty: feasibility and potential clinical advantages, J. Thorac. Cardiovasc. Surg. 120 (2000) 999–1005.
[17] J.G. Shake, P.J. Gruber, W.A. Baumgartner, G. Senechal, J. Meyers, J.M. Redmond, M.F. Pittenger, B.J. Martin, Mesenchymal stem cell implantation in a swine myocardial infarct model: engraftment and functional effects, Ann. Thorac. Surg. 73 (2002) 1919–1925 (discussion 1926).
[18] K.L. Moore, T.V.N. Persaud, The Developing Human: Clinically Oriented Embryology, Saunders, Philadelphia, Pa., 2003.
[19] K. Igura, X. Zhang, K. Takahashi, A. Mitsuru, S. Yamaguchi, T.A. Takashi, Isolation and characterization of mesenchymal progenitor cells from chorionic villi of human placenta, Cytotherapy 6 (2004) 543–553.
[20] X. Zhang, A. Mitsuru, K. Igura, K. Takahashi, S. Ichinose, S. Yamaguchi, T.A. Takahashi, Mesenchymal progenitor cells derived from chorionic villi of human placenta for cartilage tissue engineering, Biochem. Biophys. Res. Commun. 340 (2006) 944–952.
[21] J. Paquin, B.A. Danalache, M. Jankowski, S.M. McCann, J. Gutkowska, Oxytocin induces differentiation of P19 embryonic stem cells to cardiomyocytes, Proc. Natl. Acad. Sci. U. S. A. 99 (2002) 9550–9555.
[22] M. Terai, T. Uyama, T. Sugiki, X.K. Li, A. Umezawa, T. Kiyono, Immortalization of human fetal cells: the life span of umbilical cord blood-derived cells can be prolonged without manipulating p16INK4a/RB braking pathway, Mol. Biol. Cell 16 (2005) 1491–1499.
[23] D.J. Prockop, I. Sekiya, D.C. Colter, Isolation and characterization of rapidly self-renewing stem cells from cultures of human marrow stromal cells, Cytotherapy 3 (2001) 393–396.
[24] I. Potapova, A. Plotnikov, Z. Lu, P. Danilo Jr., V. Valiunas, J. Qu, S. Doronin, J. Zuckerman, I.N. Shlapakova, J. Gao, Z. Pan, A.J. Herron, R.B. Robinson, P.R. Brink, M.R. Rosen, I.S. Cohen, Human mesenchymal stem cells as a gene delivery system to create cardiac pacemakers, Circ. Res. 94 (2004) 952–959.
[25] C. Badorff, R.P. Brandes, R. Popp, S. Rupp, C. Urbich, A. Aicher, I. Fleming, R. Busse, A.M. Zeiher, S. Dimmeler, Transdifferentiation of blood-derived human adult endothelial progenitor cells into functionally active cardiomyocytes, Circulation 107 (2003) 1024–1032.
[26] K. Matsuura, H. Wada, T. Nagai, Y. Iijima, T. Minamino, M. Sano, H. Akazawa, J.D. Molkentin, H. Kasanuki, I. Komuro, Cardiomyocytes fuse with surrounding noncardiomyocytes and reenter the cell cycle, J. Cell Biol. 167 (2004) 351–363.
[27] C.H. Cui, T. Uyama, K. Miyado, M. Terai, S. Kyo, T. Kiyono, A. Umezawa, Menstrual blood-derived cells confer human dystrophin expression in the murine model of duchenne muscular dystrophy via cell fusion and myogenic transdifferentiation, Mol. Biol. Cell 18 (2007) 1586–1594.
[28] T. Mori, T. Kiyono, H. Imabayashi, Y. Takeda, K. Tsuchiya, S. Miyoshi, H. Makino, K. Matsumoto, H. Saito, S. Ogawa, M. Sakamoto, J. Hata, A. Umezawa, Combination of hTERT and bmi-1, E6, or E7 induces prolongation of the life span of bone marrow stromal cells from an elderly donor without affecting their neurogenic potential, Mol. Cell. Biol. 25 (2005) 5183–5195.
[29] J. Kohyama, H. Abe, T. Shimazaki, A. Koizumi, K. Nakashima, S. Gojo, T. Taga, H. Okano, J. Hata, A. Umezawa, Brain from bone: efficient "meta-differentiation" of marrow stroma-derived mature osteoblasts to neurons with Noggin or a demethylating agent, Differentiation 68 (2001) 235–244.
[30] K.D. Lee, T.K. Kuo, J. Whang-Peng, Y.F. Chung, C.T. Lin, S.H. Chou, J.R. Chen, Y.P. Chen, O.K. Lee, In vitro hepatic differentiation of human mesenchymal stem cells Hepatology 40 (2004) 1275–1284.
[31] I. Komuro, S. Izumo, Csx: a murine homeobox-containing gene specifically expressed in the developing heart, Proc. Natl. Acad. Sci. U. S. A. 90 (1993) 8145–8149.
[32] I. Shiojima, I. Komuro, T. Mizuno, R. Aikawa, H. Akazawa, T. Oka, T. Yamazaki, Y. Yazaki, Molecular cloning and characterization of human cardiac homeobox gene CSX1, Circ. Res. 79 (1996) 920–929.
[33] Y. Yamada, K. Sakurada, Y. Takeda, S. Gojo, A. Umezawa, Single-cell-derived mesenchymal stem cells overexpressing Csx/Nkx2.5 and GATA4 undergo the stochastic cardiomyogenic fate and behave like transient amplifying cells, Exp. Cell Res. 313 (2007) 698–706.
[34] F. Ishikawa, Cellular senescence, an unpopular yet trustworthy tumor suppressor mechanism, Cancer Sci. 94 (2003) 944–947.

STEM CELLS

TISSUE-SPECIFIC STEM CELLS

# The Significant Cardiomyogenic Potential of Human Umbilical Cord Blood-Derived Mesenchymal Stem Cells In Vitro

NOBUHIRO NISHIYAMA,[a] SHUNICHIRO MIYOSHI,[a,b] NAOKO HIDA,[a,c] TARO UYAMA,[c] KAZUMA OKAMOTO,[d] YUKINORI IKEGAMI,[a] KENJI MIYADO,[c] KAORU SEGAWA,[f] MASANORI TERAI,[c] MICHIIE SAKAMOTO,[e] SATOSHI OGAWA,[a] AKIHIRO UMEZAWA[c]

[a]Cardiopulmonary Division, Keio University School of Medicine, Tokyo, Japan; [b]Keio University School of Medicine, Institute for Advanced Cardiac Therapeutics, Tokyo, Japan; [c]Department of Reproductive Biology and Pathology, National Research Institute for Child Health and Development, Tokyo, Japan; [d]Department of Surgery, [e]Department of Pathology, and [f]Department of Microbiology and Immunology, Keio University School of Medicine, Tokyo, Japan

**Key Words.** Physiology • Transplantation • Action potentials • Cells • Heart failure

## ABSTRACT

**We tested the cardiomyogenic potential of the human umbilical cord blood-derived mesenchymal stem cells (UCBMSCs). Both the number and function of stem cells may be depressed in senile patients with severe coronary risk factors. Therefore, stem cells obtained from such patients may not function well. For this reason, UCBMSCs are potentially a new cell source for stem cell-based therapy, since such cells can be obtained from younger populations and are being routinely utilized for clinical patients. The human UCBMSCs ($5 \times 10^3$ per cm$^2$) were cocultured with fetal murine cardiomyocytes ([CM] $1 \times 10^5$ per cm$^2$). On day 5 of cocultivation, approximately half of the green fluorescent protein (GFP)-labeled UCBMSCs contracted rhythmically and synchronously, suggesting the presence of electrical communication between the UCBMSCs. The fractional shortening of the contracted UCBMSCs was 6.5% ± 0.7% ($n$ = 20). The UCBMSC-derived cardiomyocytes stained positive for cardiac troponin-I (clear striation +) and connexin 43 (diffuse dot-like staining at the margin of the cell) by the immunocytochemical method. Cardiac troponin-I positive cardiomyocytes accounted for 45% ± 3% of GFP-labeled UCBMSCs. The cardiomyocyte-specific long action potential duration (186 ± 12 milliseconds) was recorded with a glass microelectrode from the GFP-labeled UCBMSCs. CM were observed in UCBMSCs, which were cocultivated in the same dish with mouse cardiomyocytes separated by a collagen membrane. Cell fusion, therefore, was not a major cause of CM in the UCBMSCs. Approximately half of the human UCBMSCs were successfully transdifferentiated into cardiomyocytes in vitro. UCBMSCs can be a promising cellular source for cardiac stem cell-based therapy.** STEM CELLS *2007;25:2017–2024*

Disclosure of potential conflicts of interest is found at the end of this article.

## INTRODUCTION

Autologous stem cells are believed to be a potential cellular source for stem cell-based therapy, since they have the ability to proliferate and differentiate into cardiomyocytes [1–4]. Many types of cells, such as embryonic stem cells [5, 6], myoblasts [7, 8], bone marrow hematopoietic cells [9, 10], and mesenchymal stem cells (MSCs) [11–13], have been transplanted to restore damaged heart function in animal models. Autologous mononuclear cells [14–17] and myoblasts [18] have been injected into ischemic hearts clinically to improve impaired cardiac function. Despite the dramatic improvement of cardiac function by the stem-cell-based therapy in the animal model [10, 19], only modest effects were observed in the clinical study [14–17, 20]. One of the reasons for this may have been the extremely low rate of cardiomyogenesis of the stem cells in vitro and in vivo [2, 13, 21]. Therefore, the improvement of cardiac function may have been due to grafted stem cell-induced neovascularization [13, 22] and/or the paracrine effect [23]. Another reason may have been the ages and disease histories of the patients. Recent papers have shown that the number and function of the circulating stem cells were depressed in older patients and in patients with diabetes mellitus [24, 25], suggesting that stem cells obtained from patients with coronary risk factors may not function well. This suggests limits to the utilization of autologous stem cells for the ischemic cardiomyopathy patient. On the other hand, in order to do allogenic stem cell transplantation, human leukocyte antigen (HLA)-type matching is very important for the stable survival of grafts. Therefore, the sample, which can be noninvasively collected from many volunteers, is a desirable source of stem cells due to the ease of establishing cell banks that can store all HLA-types.

Recently, umbilical cord blood (UCB) banking for transplantation of hematopoietic stem cells has become popular [26]. If we can utilize UCB for heart failure patients, we can utilize this UCB stem cell bank network system immediately. UCB-derived stem cells may be superior to marrow-derived stem cells because they are obtained from infants. UCB contains circulating stem/progenitor cells, and the cells contained in UCB are

Correspondence: Shunichiro Miyoshi, M.D., Ph.D., Cardiopulmonary Division of Keio University School of Medicine, 35-Shinanomachi Shinjuku-ku, Tokyo 160-8582, Japan. Telephone: +81-3-3353-1211 (ext. 62310); Fax: +81-3-3353-2502; e-mail: smiyoshi@cpnet.med.keio.ac.jp Received October 23, 2006; accepted for publication May 6, 2007; first published online in STEM CELLS *EXPRESS* May 10, 2007. ©AlphaMed Press 1066-5099/2007/$30.00/0 doi: 10.1634/stemcells.2006-0662

known to be quite distinct from those contained in bone marrow and adult peripheral blood [27]. UCB transplantation has been reported to improve cardiac function [28–30]. That study, however, used a fraction of hematopoietic lineage and failed to show any clear evidence for cardiomyogenesis in vivo. In the present study, we focus on the mesenchymal lineage of UCB.

Isolation, characterization, and differentiation of clonally expanded umbilical cord blood-derived mesenchymal stem cells (UCBMSCs) have been reported [31, 32]. UCBMSCs have been found to have multipotency, and the immunophenotype of the clonally expanded cells is consistent with that reported for bone marrow mesenchymal stem cells [33, 34]. Kim et al. [35] showed modest but significant functional recovery of impaired cardiac function by transplantation of human unrestricted somatic stem cells obtained from umbilical cord blood that expressed mesenchymal cell surface markers [34]; therefore, mesenchymal lineage of the cells obtained from UCB may have potential therapeutic advantage in cardiac stem cell therapy. However, in vitro [33] and in vivo [34, 35], cardiomyogenic transdifferentiation ability have not yet been extensively studied. In the present study, we find that UCBMSCs have a strong potential for cardiomyogenic transdifferentiation.

## MATERIALS AND METHODS

### Isolation and Cell Culture of UCBMSCs

The detailed isolation method has been described previously [33]. A few colonies were found in the culture dish bottom 1 month after the collected cells were cultured in Dulbecco's modified Eagle's medium (DMEM) with 10% fetal bovine serum (FBS). One colony was trypsinized using a colony cylinder and then used for the experiment. We designated the monoclonal cell line as UCBMSC. The cells were prepared for infection with recombinant retroviruses expressing the human telomerase reverse transcriptase (TERT), as described previously [2, 33]. Stably transduced cells with an expanded life span were designated UCBMSC-TERT. The cells were cultured for further experiments under the approval of the Ethics Committee of our institute.

### Preparation of Murine Fetal Cardiomyocytes

Fetal cardiomyocytes were obtained from the hearts of day 17 mouse fetuses [2]. Hearts were minced with scissors and washed with phosphate-buffered saline (PBS), and the minced hearts were incubated in PBS with 0.05% trypsin and 0.25 mM EDTA (ethylenediamine-*N*,*N*,*N*′,*N*′-tetraacetic acid) (Invitrogen, Carlsbad, CA, http://www.invitrogen.com) for 10 minutes at 37°C. After DMEM supplemented with 10% FBS was added, the cardiomyocytes were centrifuged at 1,000 rpm for 5 minutes. The pellet was then resuspended in 10 ml of DMEM with 10% FBS and incubated on glass dishes for 1 hour to separate the cardiomyocytes from fibroblasts. The floating cardiomyocytes were collected and replated at $1 \times 10^5$ per $cm^2$.

### Coculture System of UCBMSCs/UCBMSCs-TERT and Murine Fetal Cardiomyocytes

We employed a coculture system with fetal cardiomyocytes to induce cardiac transdifferentiation, since in vitro simulation of the heart by the environment has been shown to be an efficient means of inducing the transdifferentiation of human marrow-derived MSC [2]. Cryopreserved UCBMSCs and UCBMSCs-TERT were used for the experiment. After thawing, the cells were cultured for at least two passages to stabilize the condition of the cell before the cardiomyogenic induction. UCBMSCs and UCBMSCs-TERT were labeled with enhanced green fluorescent protein (GFP) by recombinant adenovirus transfection as described previously [2]. These cells were then exposed to 3 μM 5-azacytidine (5-azaC; Sigma-Aldrich, St. Louis, http://www.sigmaaldrich.com) for 24 hours to induce cell transdifferentiation or were left untreated. Then, $5 \times 10^3$ per $cm^2$ of the cells were plated on the murine cardiomyocyte. The images were stored using a digital video system. The cell contraction was analyzed using a homemade image edge detection program made using Igor Pro 4 (WaveMetrics Inc., Portland, OR, http://www.wavemetrics.com). We administered 10 μM caffeine, 10 μM verapamil, or 1 μM thapsigargin to observe contraction of differentiated UCBMSCs.

### Immunocytochemistry

A laser confocal microscope (FV1000; Olympus, Tokyo, http://www.olympus-global.com) was used for immunocytochemical analysis. The UCBMSCs and UCBMSCs-TERT were stained with mouse monoclonal anti-human cardiac troponin-I antibody (number 4T21 Lot 98/10-T21-C2; HyTest, Turku, Finland, http://www.hytest.fi) diluted 1:300, monoclonal anti-α actinin antibody (Sigma) diluted 1:300, or anti-connexin 43 antibody (Sigma) diluted 1:300. Nuclei were stained with 4′-6-diamidino-2-phenylindole (Wako Chemical, Osaka, Japan, http://www.wako-chem.co.jp/english) at 1:300. tetramethylrhodamine iso-thiocyanate (TRITC)-conjugated goat anti-mouse IgG (Sigma), TRITC-conjugated goat anti-rabbit IgG (Sigma), and Cy5-conjugated goat anti-mouse IgG (Chemicon, Temecula, CA, http://www.chemicon.com) were used as secondary antibodies.

### Calculation of Induction Rate

After 1 week, UCBMSCs and UCBMSCs-TERT cultivated with or without murine fetal cardiomyocytes were detached from the dish by 0.1% trypsin and 0.25 mM EDTA for 5 minutes. The mass of cells obtained was then dissociated by 0.5% collagenase type-II (Worthington Biochemical, Lakewood, NJ, http://www.worthington-biochem.com) and 10 mM 2,3-butanedione monoxime (Sigma)-containing culture medium for 20–60 minutes. The isolated cells were seeded on poly-L-lysine coated dishes and stained. A confocal laser microscope was used to examine the cells. The cardiomyogenic induction rate was calculated as the fraction of human cardiac troponin-I-positive cells in the GFP-positive cells. The rate was calculated as the average from more than 10 separate experiments.

### Examination of Chromosomes of UCBMSCs and Murine Cell Chimeras

Chromosomes from UCBMSCs cocultivated with murine cardiomyocyte for 1 week were stained by using a human chromosome-specific probe and a mouse chromosome-specific probe (Chromosome Science Labo, Hokkaido, Japan) and spectral karyotyping with fluorescence in situ hybridization (FISH) chromosome painting technique (Spectral Imaging, Vista, CA, http://www.spectral-imaging.com), according to the manufacturer's protocol.

### Coculture of UCBMSCs-TERT and Murine Fetal Cardiomyocytes Separated by a Collagen Membrane

UCBMSCs-TERT and murine fetal cardiomyocytes were cocultured separately within the same dish. The murine fetal cardiomyocytes were seeded on top of a floating collagen film (CM-6; Koken, Tokyo, http://www.kokenmpc.co.jp/english), and the UCBMSCs-TERT were seeded on the bottom of the film. These two types of cells were, therefore, separated by a high-density atelocollagen film with a thickness of 30–40 μm, as shown in Figure 5E, that is permeable only for small molecules, less than 5,000 molecular weight (MW). After 1 week of cocultivation, the cells were analyzed immunocytochemically.

### RNA Extraction and Reverse Transcriptase-Polymerase Chain Reaction

Total RNA was extracted from the UCBMSCs and UCBMSCs-TERT with RNeasy (Qiagen, Hilden, Germany, http://www1.qiagen.com). Human cardiac RNA was purchased (Clontech, Palo Alto, CA, http://www.clontech.com). RNA for reverse transcription-polymerase chain reaction (RT-PCR) was converted to cDNA with a first-strand cDNA synthesis kit (GE Healthcare, Bucking-

hamshire, U.K., http://www.gehealthcare.com) according to the manufacturer's recommendations. RT-PCR was performed by using primers for the following genes: Csx/Nkx-2.5, GATA4; cardiac hormones: human atrial natriuretic peptide (hANP), human brain natriuretic peptide (hBNP): cardiac structural proteins: cardiac troponin-I, cardiac troponin T, myosin heavy chain (MHC), myosin light chain-2a (MLC2a), cardiac-actin; ion channel: hyperpolarization-activated cyclic nucleotide-gated potassium channel 2 (HCN2); and 18s rRNA (18s rRNA was used as an internal control). PCR primers were prepared such that they would amplify the human but not the mouse genes [2] (supplemental online Table 1).

### Flow Cytometric Analysis

Cells were detached and stained for 30 minutes at 4°C with primary antibodies and immunofluorescent secondary antibodies. After washing, the cells were analyzed using a FACScan (BD Biosciences, San Diego, http://www.bdbiosciences.com), and the data were analyzed with the CellQuest software (BD Sciences). Antibodies (anti-human CD13, CD14, CD24, CD29, CD31, CD34, CD44, CD45, CD54, CD55, CD59, CDw90, CD105, CD117, CD133, CD140a, CD157, CD164, CD166, Flk-1, SSEA-1, SSEA-3, and SSEA-4) were purchased from Beckman Coulter (Fullerton, CA, http://www.beckmancoulter.com), Immunotech (Luminy, France, http://www.beckmancoulter.com/products/pr_immunology.asp), Cytotech (Hellebaek, Denmark, http://www.cytotech.dk), Santa Cruz Biotechnology Inc. (Santa Cruz, CA, http://www.scbt.com), RDI (Concord, MA http://www.researchd.com), and Pharmingen Pharmaceutical Co. (San Diego).

### Electrophysiological Experiment

Action potentials (APs) from the spontaneously beating GFP-positive UCBMSCs and UCBMSCs-TERT were recorded by use of standard microelectrodes, as described previously [2]. After the APs of the targeted cells were recorded, the dye (Alexa 568) was injected by electrophoresis (−5 nA for 10–20 seconds) to confirm the recorded APs obtained from GFP-positive cells. The extent of dye transfer was monitored under a fluorescent microscope.

## RESULTS

### Cardiomyogenic Transdifferentiation of UCBMSCs and UCBMSCs-TERT

On day 3 after starting the cocultivation, a few GFP-positive UCBMSCs and UCBMSCs-TERT started to contract ($n$ = 68). On day 7, the beating of the murine cardiomyocytes stopped, whereas approximately half of the GFP-positive UCBMSCs and UCBMSCs-TERT beat strongly in a synchronized manner.

Immunocytochemistry revealed that a significant number of UCBMSCs and UCBMSCs-TERT expressing GFP were stained positive by the anti-human cardiac troponin-I antibody (Fig. 1A–1E, supplemental online Fig. 1A–1H). A clear striation pattern of cardiac troponin-I staining of UCBMSCs can be observed in higher magnification view (Fig. 1). Interestingly, troponin-I staining and GFP were observed alternately in a striated manner, suggesting that the troponin-I was expressed in the GFP-positive cells (Fig. 1 E). Clear striations were observed with red fluorescence of α-actinin in the differentiated UCBMSCs and UCBMSCs-TERT (Fig. 2B, 2H). Arrays of cardiomyocytes can be frequently observed (Fig. 2H). Connexin 43 staining (Fig. 2C, 2I) showed a clear and diffuse pattern around the margin of each GFP-positive cardiomyocyte, suggesting that these human transdifferentiated cardiomyocytes have tight electrical coupling with each other.

We also calculated the percentage of the human cardiac troponin-I-positive cells to determine the cardiomyogenic transdifferentiation rate of UCBMSCs and UCBMSCs-TERT. Since there was no essential difference between the UCBMSCs and UCBMSCs-TERT, calculated data from both cell types are averaged and shown in Figure 3. Although UCBMSCs without cocultivation did not show any troponin-I expression (Fig. 3H, 3K), 45% ± 3% of UCBMSCs became positive for human cardiac troponin-I antibody as a result of the cocultivation (Fig.

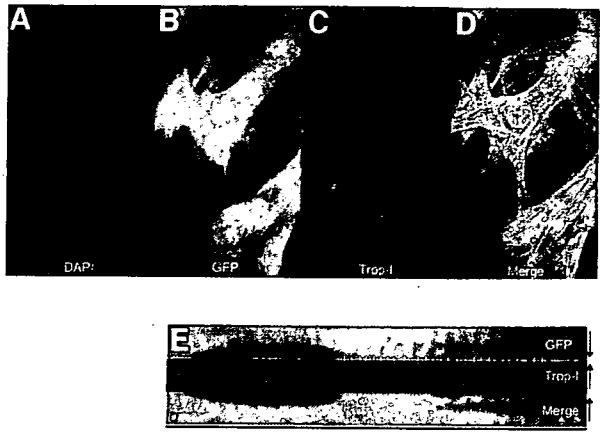


**Figure 1.** Cardiomyogenic transdifferentiation of umbilical cord blood mesenchymal stem cells. Laser confocal microscopic view of immunocytochemistry of differentiated umbilical cord blood mesenchymal stem cells with anti-cardiac troponin-I antibody. Superimposed images (Merge) of **(A–C)** are shown in **(D)**. Significant numbers of differentiated GFP-positive umbilical cord blood-derived mesenchymal stem cells (green) had troponin-I (red) in their cytoplasm (yellow as a result of "merging" **[D]**). Nuclei are stained with DAPI **([A]**, blue). Clear troponin-I (red) staining with striation pattern can be observed. GFP **([B]**, green) and Trop-I **([C]**, red) along the white line in **(C)** are magnified in panel **(E)**. Interestingly, troponin-I staining and GFP were observed alternately in a striated manner, suggesting the troponin-I expressed in the GFP-positive cells. Scale bars in the figure denote 20 μm. Abbreviations: DAPI, 4,6-diamidino-2-phenylindole; GFP, green fluorescent protein; Trop-I, troponin-I.

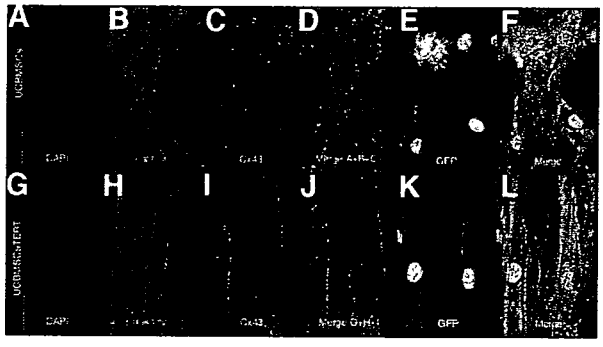


**Figure 2.** Immunocytochemical analysis of umbilical cord blood mesenchymal stem cell stained with anti-sarcomeric α-actinin and connexin 43. Laser confocal microscopic view of immunocytochemistry of differentiated umbilical cord blood mesenchymal stem cells and cells transduced with human TERT gene to prolong their life span (UCBMSCs-TERT) with anti-sarcomeric α-actinin **([B, H]**: α-actinin, red) and connexin 43 **([C, I]**: Cx43, cyan) antibody. Superimposed images (Merge) of **(A–C)** and **(G–I)** are shown in **(D)** and **(J)**, respectively. Clear striation pattern of α-actinin and diffuse Cx43 dot-like staining around the margin of the UCBMSCs were observed. These cells are GFP-positive UCBMSCs **([E, K]**: GFP, green. Merged images of **[D, E]** and **[J, K]** are **[F]** and **[L]**, respectively). Nuclei are stained with DAPI **([A, G]**, blue). It is noted that arrays of the UCBMSC-derived cardiomyocytes are sometimes observed **(J)**. Scale bars in the figure denote 50 μm. Abbreviations: DAPI, 4,6-diamidino-2-phenylindole; GFP, green fluorescent protein; UCBMSCs, umbilical cord blood mesenchymal stem cells; UCBMSCs-TERT, umbilical cord blood mesenchymal stem cells-telomerase reverse transcriptase.

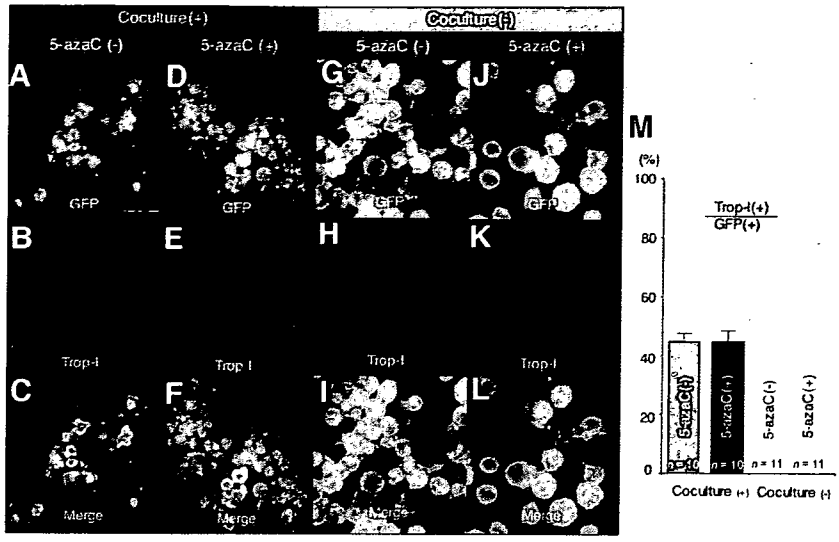


**Figure 3.** Calculation of cardiomyogenic transdifferentiation ratio of umbilical cord blood mesenchymal stem cells (UCBMSCs). **(A–L):** Representative laser confocal image of cardiac troponin-I ([**B, E, H, K**]: Trop-I, red) staining to calculate cardiomyogenic transdifferentiation rate of UCBMSCs. Upper bar denotes the culture conditions for each panel presented bellow. (Coculture: cocultivation with fetal murine cardiomyocyte, 5-azaC: pretreatment with 5-azacytidine.) Approximately half of the isolated GFP-positive UCBMSCs ([**A, D**]: GFP, green) stained positive for Trop-I (**B, E**) as a result of coculture. A superimposed image of (**A**) + (**B**) and (**D**) + (**E**) are shown in (**C**) and (**F**), respectively. On the other hand, UCBMSCs (**G, J**) do not show any Trop-I staining (**H, K**). Scale bars in the figure denote 50 $\mu$m. The cardiomyogenic transdifferentiation rate of UCBMSCs was defined as the percentage of Trop-I-positive cells in the GFP-positive cells. Measured data were averaged and are shown (**M**). Error bars denote SEM ($n$ = 20). Abbreviations: 5-azaC, 5-azacytidine; GFP, green fluorescent protein; Trop-I, troponin-I.

3B, 3E). It is noted that cardiomyogenic transdifferentiation could be observed in the cocultivated UCBMSCs and UCBMSCs-TERT without any 5-azaC pretreatment.

## Cell Fusion-Independent Cardiomyogenic Transdifferentiation

Cell fusion has been shown to be quite a rare phenomenon [4, 36]; however, it may contribute to the generation of cardiomyocytes in our system. Nuclear fusion between the cocultivated UCBMSCs-TERT and fetal murine cardiomyocytes was observed in only approximately 0.09% (2/2165) of the cocultivated cells by FISH analysis (Fig. 4A–4D). In the differentiated cardiomyocyte, there is no cell having double nuclei in the isolated GFP-positive UCBMSCs. Furthermore, in cocultures of UCBMSCs-TERT with fetal murine cardiomyocytes separated by a collagen membrane (Fig. 4E), we observed beating GFP-positive cells and human cardiac troponin-I expression (Fig. 4F–4L) ($n$ = 8). Because these two cell types were not attached directly to each other, it was concluded that the cardiomyogenesis in the present study was mainly caused by the transdifferentiation of the UCBMSCs.

## Expression of Cardiomyocyte-Specific Genes and Surface Markers of UCBMSCs and UCBMSCs-TERT

We analyzed the cocultured UCBMSCs and UCBMSCs-TERT in terms of gene expression and by immunocytochemistry and electrical recording. RT-PCR was performed with primers that hybridized with human cardiomyocyte-specific genes but not with the murine orthologues (second column from the right, Fig. 5A). Differentiated UCBMSCs-TERT expressed Csx/Nkx-2.5, GATA4, hANP, hBNP, cardiac-actin, MHC, MLC2a, cardiac troponin T, cardiac troponin-I, and HCN2. Interestingly, all of the analyzed genes except for the MHC and MLC2a were expressed in UCBMSCs and UCBMSCs-TERT before the induction, implying that UCBMSCs may have cardiomyogenic potential as a default state, like CMG cells, in which Csx/Nkx-2.5 and GATA4 are constitutively expressed before induction [3]. Sequence analysis revealed that the sequences of the cDNAs matched those of the human genes.

Surface markers of the UCBMSCs-TERT were evaluated by flow cytometric analysis. The results showed that all of the

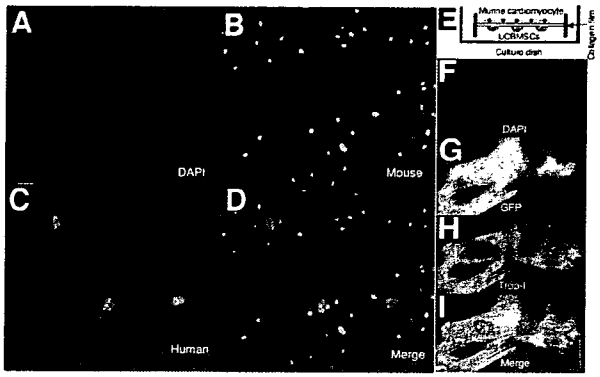


**Figure 4.** Cell fusion-independent cardiomyogenesis in UCBMSCs. **(A–D):** Representative images of fluorescent in situ hybridization for human nucleus and mouse nucleus are shown. Nuclei are stained with DAPI ([**A**]: blue). Mouse nuclei were detected as green (**B**) and human nuclei were detected as red (**C**). Superimposed image of (**A–C**) is shown in (**D**) (Merge). See text for details. **(E):** The experimental scheme is shown. The murine cardiomyocytes and UCBMSCs were cocultured on the top and the bottom of a collagen membrane, respectively. The cocultivated UCBMSCs and murine cardiomyocytes were separated by the 50-$\mu$m-thick collagen membrane. Nuclei were stained with DAPI ([**F**]: blue) and UCBMSCs were labeled with GFP ([**G**]: green). UCBMSCs were stained with anti-human cardiac troponin-I antibody ([**H**]: red), and the merged images (DAPI, GFP, Trop-I) are shown (**I**). Scale bars in the figure denote 20 $\mu$m. Abbreviations: DAPI, 4,6-diamidino-2-phenylindole; GFP, green fluorescent protein; Trop-I, troponin-I; UCBMSCs, umbilical cord blood mesenchymal stem cells.

UCBMSCs-TERT were positive for CD29 (integrin $\beta$1), CD44 (Pgp-1/Iy-24), CD54, CD55, CD59, CDw90, CD105, CD157, CD164, CD166, and SSEA-4 and negative for CD14 (a marker for macrophage and dendritic cells), CD31 (platelet endothelial cell adhesion molecule-1), CD34, CD45 (leukocyte common antigen), CD117 (c-kit), CD133, CD140a, Flk-1, SSEA-1, and SSEA-3 (Fig. 5B). Our UCBMSCs are negative for CD34, CD45, Flk-1, and CD133, thus differing from hematopoietic stem cell and from circulating endothelial progenitor cells. It is noted that our UCBMSCs are weakly positive for SSEA4 [37], an embryonic stem cell marker. Thus, UCBMSCs may be more plastic for transdifferentiation than other somatic stem cells.

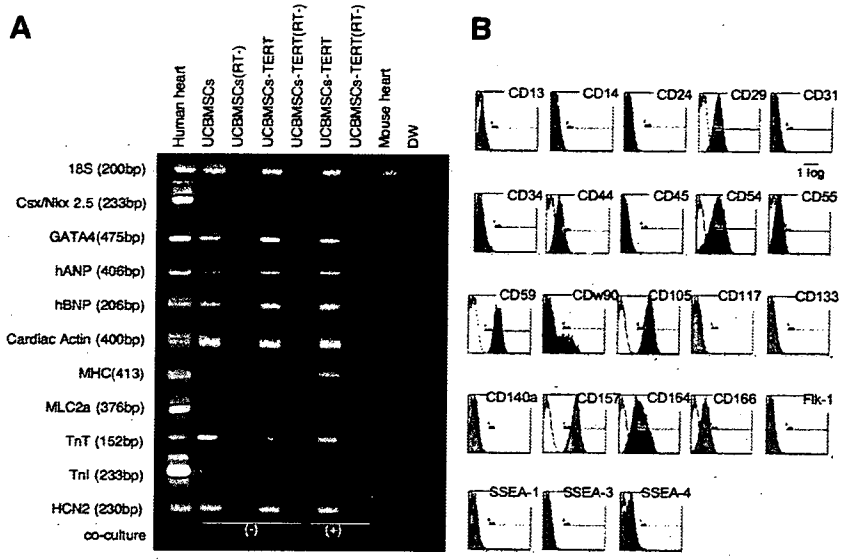


**Figure 5.** Expression of cardiomyocyte-specific genes in UCBMSCs and cell surface markers of UCBMSCs. **(A):** Expression of cardiomyocyte-specific genes in UCBMSCs and UCBMSCs-TERT. Reverse transcription-polymerase chain reaction (PCR) was performed with PCR primers with specificity for human genes encoding cardiac proteins but not for the corresponding murine genes. Only the 18S PCR primer used as a positive control reacted with both the human and murine genes. Human heart and mouse heart were used as a positive control and negative control, respectively. Almost all human cardiac genes were constitutively expressed in the default state. **(B):** Flow cytometric analysis of UCBMSCs with fluorescein isothiocyanate-coupled antibodies against the human surface antigens. Abbreviations: DW, distilled water; hANP, human atrial natriuretic peptide; hBNP, human brain natriuretic peptide; HCN2, hyperpolarization-activated cyclic nucleotide-gated potassium channel 2; MHC, myosin heavy chain; MLC2a, myosin light chain-2a; RT, reverse transcriptase; TnI, cardiac troponin I; TnT, cardiac troponin T; UCBMSCs, umbilical cord blood mesenchymal stem cells; UCBMSCs-TERT, umbilical cord blood mesenchymal stem cells-telomerase reverse transcriptase.

## Functional Analysis of Differentiated UCBMSCs and UCBMSCs-TERT In Vitro

APs were recorded from spontaneously beating GFP-positive UCBMSCs and UCBMSCs-TERT. Alexa 568 was injected into cells via a recording microelectrode to stain the cells and confirm that the APs were generated by GFP-positive UCBMSCs (Fig. 6A, 6C). Since the dye did not diffuse into the murine cardiomyocytes, there were no tight cell-to-cell heterologous connections, that is, gap junctions. In most experiments, Alexa 568 diffused into the GFP-positive adjacent UCBMSCs and UCBMSCs-TERT, suggesting that homologous cell-to-cell connections had been established within 1 week after the start of cocultivation. The APs obtained from UCBMSCs and UCBMSCs-TERT showed clear cardiomyocyte-specific sustained plateaus. It was, therefore, concluded that they were the APs of cardiomyocytes, not of smooth muscle, nerve cells, or skeletal muscle (Fig. 6B, 6D). The measured parameters of the recorded APs were averaged (Fig. 6E). UCBMSCs and UCBMSCs-TERT did not have a marked pacemaker potential and had the character of working cardiomyocytes or ordinary cardiomyocytes. The rhythm of almost all of the UCBMSCs and UCBMSCs-TERT had become regular at 1 week. The fractional shortening (% FS) of the UCBMSCs and UCBMSCs-TERT was analyzed (Fig. 6F–6I) using a cell edge detection program. The GFP-positive cells contracted simultaneously within the whole visual field, suggesting tight electrical communication. There was no difference of % FS between the UCBMSCs and UCBMSCs-TERT. The % FS was augmented significantly by the administration of caffeine and inhibited by the administration of verapamil or thapsigargin (Fig. 7).

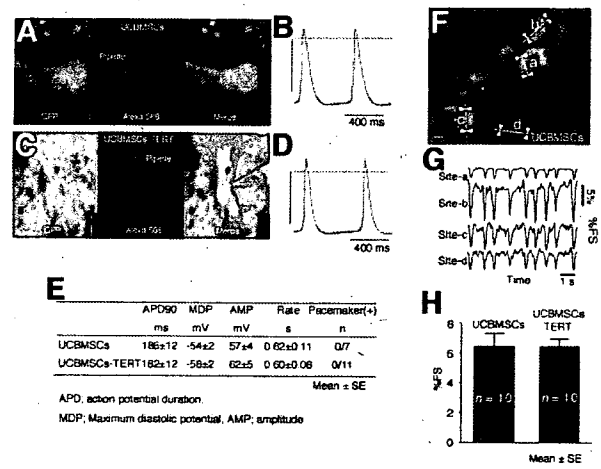


**Figure 6.** Functional analysis of UCBMSCs and UCBMSCs-TERT. Representative fluorescent microscopic images during action potential (AP) recording are shown **(A, C)**. Immediately after the AP recordings, alexa568 dye (red) was injected into the cell via the same recording electrode to confirm that the recorded AP was obtained from GFP-positive UCBMSCs. **(B, D):** Representative APs obtained from **(A)** and **(C)** respectively. The dotted line denotes the 0 mV level and the vertical line denotes 50 mV. **(E):** The measured AP parameters were averaged and are shown. **(F):** A representative still image from cell motion analysis is shown. The white arrowheads point to the automatically detected cell edge. The detected fractional shortening along the white line obtained from site-a, -b, -c, -d **(G)**. **(H):** The measured % FS was averaged and is shown. Abbreviations: AMP, amplitude; APD, action potential duration; % FS, fractional shortening; GFP, green fluorescent protein; MDP, maximum diastolic potential; ms, milliseconds; s, second; UCBMSCs, umbilical cord blood mesenchymal stem cells; UCBMSCs-TERT, umbilical cord blood mesenchymal stem cells-telomerase reverse transcriptase.

# DISCUSSION

## Physiologically Functioning Cardiomyocytes Can Be Generated from UCBMSCs In Vitro

Compared with the cardiomyogenic differentiation efficiency of the marrow-derived MSC (0.3%) [2], a significant number of the UCBMSCs transdifferentiated into cardiomyocytes in vitro in the present study. Generated cardiomyocytes showed physiologically functioning ability, that is, cardiomyocyte-specific

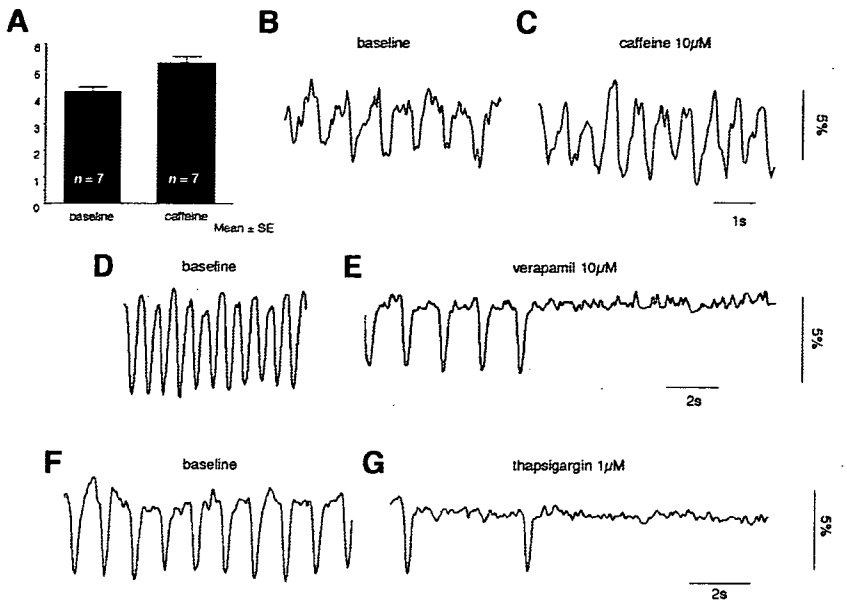


**Figure 7.** The effect of the drug administration on contraction of differentiated umbilical cord blood mesenchymal stem cells (UCBMSCs). The detected fractional shortening (% FS) of the differentiated UCBMSCs before and after the administration of caffeine (**A–C**), verapamil (**D, E**), and thapsigargin (**F, G**) are shown. The caffeine slightly increased the beating rate and increased the % FS significantly (**A**). On the other hand, immediately after the administration of verapamil (**D**) or thapsigargin (**F**), the beating rate decreased, then ceased (**E, G**). Abbreviation: s, second.

APs with long duration (more than 100 milliseconds) and spontaneous contraction. The fact that each UCBMSC beats in a synchronized manner and the fact of the diffuse connexin 43 staining together suggest the formation of tight electrical coupling among the UCBMSCs. In our previous paper, we used the cells immediately after being quickly thawed from cryopreserved UCBMSCs, then failed to observe cardiomyogenic transdifferentiation in the small number of observations [33]. Recently, however, we felt at least two passages should be required to stabilize and regain cardiomyogenic transdifferentiation ability in UCBMSCs and our several cell lines.

## Highly Cardiomyogenic Differentiation Potential

In the marrow-derived stem cell, mesenchymal lineage has a cardiomyogenic transdifferentiation potential [2, 3]; hematopoietic cell lineage does not [21]. This implies that mesenchymal lineage of the cell in UCB might have the ability to transdifferentiate into cardiomyocytes. Several in vivo experiments using UCB have shown feasible effects in restoring cardiac function in the myocardial infarction model [28–30]. However, these experiments used CD34+ or CD133+ hematopoietic lineage of the cell in UCB and failed to show any clear evidence of cardiomyogenesis. Surface marker analysis revealed UCBMSCs as differing from hematopoietic stem cells and from circulating endothelial progenitor cells. Kögler et al. [34] reported that stem cells obtained from UCB, so-called unrestricted somatic stem cells (USSCs), have a pluripotent differential potential with a similar surface marker pattern, that is, negative for CD34 and CD45 and positive for CD29 and CD44, that is typical for mesenchymal cells. Furthermore, Kim et al. [35] showed that USSCs improved impaired cardiac function in vivo. Although the two papers showed modest evidence for cardiomyogenic potential of USSCs in vivo, experiments had not been extensively done to show the evidence of cardiac transdifferentiation. Finally, these papers failed to show clear evidence for cell fusion-independent cardiomyogenesis and efficiency of cardiomyogenic differentiation. In the present study, we show significant potential of cell fusion-independent cardiomyogenesis of UCBMSCs.

## Comparisons with Other Stem Cells for Cardiology

Cardiac precursor cells (CPCs) [38] should be a promising stem cell source for cardiac regeneration therapy. However, CPCs failed to differentiate to the physiologically functioning cardiomyocyte in vitro, and cardiomyogenic differentiation efficiency in vivo was 29%–40%. Thus, cardiomyogenic differentiation efficiency might not be so markedly high compared with the UCBMSCs. Moreover, it is very difficult to match the donor-recipient HLA-type, and there is still a longstanding ethical problem. An embryonic stem cell is a pluripotential stem cell that has a cardiomyogenic differentiation potential. But there are still critical underlying problems, that is, teratoma formation [39], genomic alteration in long-term culture [40], and the ethical problem. Differing from embryonic stem cells, our RT-PCR data suggest constitutive expression of Nkx2.5/Csx and GATA4 and other cardiac structure mRNA with the ability of self-renewal. This suggests that some population of the UCBMSCs has cardiomyogenic potential as the default state, and they may be termed cardiac precursor cells in light of their biological features. Recently, we reported that human endometrial gland-derived mesenchymal cells also have a high cardiomyogenic potential [41]. This suggests that they may be a stem cell source for heart disease. However, for male patients, there is no choice for autologous transplantation of this cell and no running stem cell bank for this cell. On the other hand, if UCBMSCs were isolated and frozen at the time of birth, they could later be thawed for use by the donor who required cardiac stem cell therapy at a later age. Furthermore, UCB banking has played a major role for hematopoietic stem cell transplantation for leukemia treatment. If we utilize a world-wide UCB bank system for cardiac stem cell therapy, we may be able to utilize UCBMSCs for cardiac stem cell therapy in the near future. Since several reports showed that mesenchymal cells cause immunological tolerance [42–44], we speculate that only a minimum administration of immunosuppressive agents may be sufficient to control rejection of the allogenic UCBMSC transplantation, if we match the other MHC antigen by utilizing the stem cell bank system.

## Study Limitations

From a single stem cell we can obtain approximately $2^{32}$ cells with extremely high cardiomyogenic potential; however, the number of MSCs in the UCB is quite low, as was described previously [33, 34]. Thus, further experiments should be done to establish a method to collect the UCBMSCs efficiently. The transfection of the TERT gene may alter the phenotype of UCBMSCs to some extent. However, TERT-gene transfection was not essential for causing cardiomyogenic differentiation of UCBMSCs, and there was no essential difference between the UCBMSCs and UCBMSCs-TERT in the present study.

Our in vitro cardiomyogenic induction system provided a substantial environmental factor to cause cardiomyogenic transdifferentiation of UCBMSCs in vitro; however, specific key factors (e.g., humoral factors) for cardiomyogenesis were still unclear. It is still undetermined whether such key factors for cardiomyogenesis are sufficiently provided by the surrounding host heart when UCBMSCs are engrafted in vivo. We believe that the definition of these specific factors in vitro should be extremely important to improve cardiomyogenesis in situ; therefore, in the present study, we focused on in vitro cardiomyogenesis of UCBMSCs.

Cell fusion is a rare phenomenon (0.6%–0.05%) [36], and the frequency of nuclear fusion was low (0.1%) in the present study. On the other hand, the cardiomyogenic differentiation efficiency of UCBMSCs was extremely high (44.9% ± 3.6%). Furthermore, a 40-μm-thick atelocollagen membrane is not permeable for molecules larger than 5,000 MW, and no cell migration from the top of the membrane to the bottom was observed in our culture condition. On this basis, we concluded that cell fusion did not play a major role in the UCBMSC-derived cardiomyogenesis in the present study.

## Summary

Our major findings in the present study are: (a) for the first time, physiologically functioning cardiomyocytes were transdifferentiated from human UCBMSCs in vitro; (b) the observed cardiomyogenic transdifferentiation, independent of cell fusion, was approximately 44.9% ± 3.6% of UCBMSCs; and (c) cocultivation with fetal murine cardiomyocytes alone without other transdifferentiation factors, that is, 5-azaC, is sufficient for cardiomyogenesis in our system. Therefore, UCBMSCs may be a promising cellular source for cardiac stem cell-based therapy, by which cardiomyogenesis can be expected.

## Disclosure of Potential Conflicts of Interest

The authors indicate no potential conflicts of interest.

## References


1 Koyanagi M, Haendeler J, Badorff C et al. Non-canonical Wnt signaling enhances differentiation of human circulating progenitor cells to cardiomyogenic cells. J Biol Chem 2005:280:16838–16842.
2 Takeda Y, Mori T, Imabayashi H et al. Can the life span of human marrow stromal cells be prolonged by bmi-1, E6, E7, and/or telomerase without affecting cardiomyogenic differentiation? J Gene Med 2004;6: 833–845.
3 Makino S, Fukuda K, Miyoshi S et al. Cardiomyocytes can be generated from marrow stromal cells in vitro. J Clin Invest 1999;103: 697–705.
4 Iijima Y, Nagai T, Mizukami M et al. Beating is necessary for transdifferentiation of skeletal muscle-derived cells into cardiomyocytes. FASEB J 2003;17:1361–1363.
5 Klug MG, Soonpaa MH, Koh GY et al. Genetically selected cardiomyocytes from differentiating embronic stem cells form stable intracardiac grafts. J Clin Invest 1996;98:216–224.
6 Min JY, Yang Y, Converso KL et al. Transplantation of embryonic stem cells improves cardiac function in postinfarcted rats. J Appl Physiol 2002:92:288–296.
7 Ghostine S, Carrion C, Souza LC et al. Long-term efficacy of myoblast transplantation on regional structure and function after myocardial infarction. Circulation 2002;106(12 suppl 1):I131–I136.
8 Taylor DA, Atkins BZ, Hungspreugs P et al. Regenerating functional myocardium: Improved performance after skeletal myoblast transplantation. Nat Med 1998;4:929–933.
9 Jackson KA, Majka SM, Wang H et al. Regeneration of ischemic cardiac muscle and vascular endothelium by adult stem cells. J Clin Invest 2001:107:1395–1402.
10 Orlic D, Kajstura J, Chimenti S et al. Bone marrow cells regenerate infarcted myocardium. Nature 2001;410:701–705.
11 Wang JS, Shum-Tim D, Galipeau J et al. Marrow stromal cells for cellular cardiomyoplasty: Feasibility and potential clinical advantages. J Thorac Cardiovasc Surg 2000;120:999–1005.
12 Shake JG, Gruber PJ, Baumgartner WA et al. Mesenchymal stem cell implantation in a swine myocardial infarct model: Engraftment and functional effects. Ann Thorac Surg 2002;73:1919–1925.
13 Gojo S, Gojo N, Takeda Y et al. In vivo cardiovasculogenesis by direct injection of isolated adult mesenchymal stem cells. Exp Cell Res 2003; 288:51–59.
14 Strauer BE, Brehm M, Zeus T et al. Repair of infarcted myocardium by autologous intracoronary mononuclear bone marrow cell transplantation in humans. Circulation 2002;106:1913–1918.
15 Hamano K, Nishida M, Hirata K et al. Local implantation of autologous bone marrow cells for therapeutic angiogenesis in patients with ischemic heart disease: Clinical trial and preliminary results. Jpn Circ J 2001;65: 845–847.
16 Assmus B, Schachinger V, Teupe C et al. Transplantation of progenitor cells and regeneration enhancement in acute myocardial infarction (TOPCARE-AMI). Circulation 2002;106:3009–3017.
17 Tse HF, Kwong YL, Chan JK et al. Angiogenesis in ischaemic myocardium by intramyocardial autologous bone marrow mononuclear cell implantation. Lancet 2003;361:47–49.
18 Menasche P, Hagege AA, Scorsin M et al. Myoblast transplantation for heart failure. Lancet 2001;357:279–280.
19 Tomita S, Li RK, Weisel RD et al. Autologous transplantation of bone marrow cells improves damaged heart function. Circulation 1999;100: II247–II256.
20 Stamm C, Westphal B, Kleine HD et al. Autologous bone-marrow stem-cell transplantation for myocardial regeneration. Lancet 2003;361:45–46.
21 Murry C, Soonpaa M, Reinecke H et al. Haematopoietic stem cells do not transdifferentiate into cardiac myocytes in myocardial infarcts. Nature 2004;428:664–668.
22 Tang YL, Zhao Q, Zhang YC et al. Autologous mesenchymal stem cell transplantation induce VEGF and neovascularization in ischemic myocardium. Regul Pept 2004;117:3–10.
23 Gnecchi M, He H, Liang O et al. Paracrine action accounts for marked protection of ischemic heart by Akt-modified mesenchymal stem cells. Nat Med 2005;11:367–368.
24 Fadini GP, Miorin M, Facco M et al. Circulating endothelial progenitor cells are reduced in peripheral vascular complications of type 2 diabetes mellitus. J Am Coll Cardiol 2005;45:1449–1457.
25 Heiss C, Keymel S, Niesler U et al. Impaired progenitor cell activity in age-related endothelial dysfunction. J Am Coll Cardiol 2005;45:1441–1448.
26 Warkentin P and Foundation for the Accreditation of Cellular Therapy. Voluntary accreditation of cellular therapies: Foundation for the Accreditation of Cellular Therapy (FACT). Cytotherapy 2003;5:299–305.
27 Mayani H, Lansdorp PM. Biology of human umbilical cord blood-derived hematopoietic stem/progenitor cells. STEM CELLS 1998;16: 153–165.
28 Hirata Y, Sata M, Motomura N et al. Human umbilical cord blood cells improve cardiac function after myocardial infarction. Biochem Biophys Res Commun 2005;327:609–614.
29 Leor J, Guetta E, Feinberg M et al. Human umbilical cord blood-derived CD133+ cells enhance function and repair of the infarcted myocardium. STEM CELLS 2006;24:772–780.
30 Ma N, Stamm C, Kaminski A et al. Human cord blood cells induce angiogenesis following myocardial infarction in NOD/scid-mice. Cardiovasc Res 2005;66:45–54.
31 Lee OK, Kuo TK, Chen WM et al. Isolation of multipotent mesenchymal stem cells from umbilical cord blood. Blood 2004;103:1669–1675.
32 Goodwin HS, Bicknese AR, Chien SN et al. Multilineage differentiation

activity by cells isolated from umbilical cord blood: Expression of bone, fat, and neural markers. Biol Blood Marrow Transplant 2001;7:581–588.
33 Terai M, Uyama T, Sugiki T et al. Immortalization of human fetal cells: The life span of umbilical cord blood-derived cells can be prolonged without manipulating p16INK4a/RB braking pathway. Mol Biol Cell 2005;16:1491–1499.
34 Kögler G, Sensken S, Airey J et al. A new human somatic stem cell from placental cord blood with intrinsic pluripotent differentiation potential. J Exp Med 2004;200:123–135.
35 Kim BO, Tian H, Prasongsukarn K et al. Cell transplantation improves ventricular function after a myocardial infarction: A preclinical study of human unrestricted somatic stem cells in a porcine model. Circulation 2005;112(suppl 9):I96–I104.
36 Matsuura K, Wada H, Nagai T et al. Cardiomyocytes fuse with surrounding noncardiomyocytes and reenter the cell cycle. J Cell Biol 2004;167: 351–363.
37 Kannagi R, Cochran N, Ishigami F et al. Stage-specific embryonic antigens (SSEA-3 and -4) are epitopes of a unique globo-series ganglioside isolated from human teratocarcinoma cells. EMBO J 1983;2:2355–2361.
38 Beltrami A, Barlucchi L, Torella D et al. Adult cardiac stem cells are multipotent and support myocardial regeneration. Cell 2003;114: 763–776.
39 Leor J, Gerecht-Nir S, Cohen S et al. Undifferentiated human embryonic stem cells are not guided to form new myocardium by transplantation into normal and infarcted heart. Paper presented at: American College of Cardiology Meeting; March 6–9, 2005; Orlando, FL.
40 Maitra A, Arking D, Shivapurkar N et al. Genomic alterations in cultured human embryonic stem cells. Nat Genet 2005;37:1099–1103.
41 Miyoshi S, Hida N, Nishiyama N et al. Human menstrual blood is a potential cell source for cardiac stem cell therapy. Paper presented at: American College of Cardiology Meeting; March 6–9, 2005; Orlando, FL.
42 Makkar RR, Price MJ, Lill M et al. Intramyocardial injection of allogenic bone marrow-derived mesenchymal stem cells without immunosuppression preserves cardiac function in a porcine model of myocardial infarction. J Cardiovasc Pharmacol Ther 2005;10:225–233.
43 Beyth S, Borovsky Z, Mevorach D et al. Human mesenchymal stem cells alter antigen-presenting cell maturation and induce T-cell unresponsiveness. Blood 2005;105:2214–2219.
44 Tsafrir A, Brautbar C, Nagler A et al. Alloreactivity of umbilical cord blood mononuclear cells: Specific hyporesponse to noninherited maternal antigens. Hum Immunol 2000;61:548–554.


See www.StemCells.com for supplemental material available online.

Molecular Biology of the Cell
Vol. 18, 1850–1860, May 2007

# R-Ras Regulates Exocytosis by Rgl2/Rlf-mediated Activation of RalA on Endosomes[D] [V]

**Akiyuki Takaya,*† Takahiro Kamio,* Michitaka Masuda,‡ Naoki Mochizuki,‡ Hirofumi Sawa,§ Mami Sato,§ Kazuo Nagashima,§ Akiko Mizutani,‖ Akira Matsuno,¶ Etsuko Kiyokawa,† and Michiyuki Matsuda*†**

*Department of Signal Transduction, Research Institute for Microbial Diseases, Osaka University, Yamadaoka, Osaka 565-0871, Japan; †Department of Pathology and Biology of Diseases, Graduate School of Medicine, Kyoto University, Kyoto 606-8501, Japan; ‡Department of Structural Analysis, National Cardiovascular Center Research Institute, Osaka 565-8565, Japan; §Laboratory of Molecular and Cellular Pathology, Graduate School of Medicine, Hokkaido University, Sapporo 060-8638, Japan; ‖Basic Medical Science and Molecular Medicine, Tokai University School of Medicine, Kanagawa 259-1193, Japan; and ¶Department of Neurosurgery, Teikyo University Ichihara Hospital, Chiba 299-0111, Japan

Submitted August 29, 2006; Revised February 16, 2007; Accepted February 28, 2007
Monitoring Editor: Mark Ginsberg

**R-Ras is a Ras-family small GTPase that regulates various cellular functions such as apoptosis and cell adhesion. Here, we demonstrate a role of R-Ras in exocytosis. By the use of specific anti-R-Ras antibody, we found that R-Ras was enriched on both early and recycling endosomes in a wide range of cell lines. Using a fluorescence resonance energy transfer-based probe for R-Ras activity, R-Ras activity was found to be higher on endosomes than on the plasma membrane. This high R-Ras activity on the endosomes correlated with the accumulation of an R-Ras effector, the Rgl2/Rlf guanine nucleotide exchange factor for RalA, and also with high RalA activity. The essential role played by R-Ras in inducing high levels of RalA activity on the endosomes was evidenced by the short hairpin RNA (shRNA)-mediated suppression of R-Ras and by the expression of R-Ras GAP. In agreement with the reported role of RalA in exocytosis, the shRNA of either R-Ras or RalA was found to suppress calcium-triggered exocytosis in PC12 pheochromocytoma cells. These data revealed that R-Ras activates RalA on endosomes and that it thereby positively regulates exocytosis.**

## INTRODUCTION

R-Ras is a Ras-family GTPase and its amino acid sequence is 55% identical to those of the classical types of Ras (H-, K-, N-Ras, collectively referred to hereafter as "Ras") (Lowe *et al.*, 1987). As is the case with the other Ras-family GTPases, R-Ras is regulated primarily by two classes of protein, guanine nucleotide exchange factor (GEF) and GTPase-activating protein (GAP). Reflecting the high sequence similarity among Ras-family GTPases, many GEFs and GAPs for R-Ras catalyze other Ras-family GTPases as well (Ohba *et al.*, 2000). Furthermore, R-Ras is known to interact with many effectors of Ras, such as Raf-1, Ral GEFs, and the p110α subunit of phosphoinositide 3-kinase (PI3K) (Rey *et al.*, 1994; Spaargaren and Bischoff, 1994; Spaargaren *et al.*, 1994; Marte *et al.*, 1997). Despite this redundancy between R-Ras and Ras, R-Ras exhibits various properties that are distinct from those of Ras. For example, R-Ras preferentially activates Ral GEFs and PI3K, but it does not activate Raf (Huff *et al.*, 1997; Rodriguez-Viciana *et al.*, 2004). The transforming activity of constitutively active R-Ras is substantially less potent than that of the constitutively active Ras (Cox *et al.*, 1994), although it should be noted that a recent report has suggested the involvement of R-Ras in human gastric cancer (Nishigaki *et al.*, 2005). Meanwhile, R-Ras is known to regulate cell adhesion, cell spreading, and phagocytosis through the activation of integrin (Zhang *et al.*, 1996; Keely *et al.*, 1999; Berrier *et al.*, 2000; Self *et al.*, 2001). R-Ras-null mice have recently been shown to exhibit excessive vascular responses, in spite of the fact that they are otherwise normal (Komatsu and Ruoslahti, 2005). This phenotype seems to reflect higher levels of expression of R-Ras in smooth muscle cells, including blood vessel cells. The results obtained with R-Ras-null mice have also demonstrated that an R-Ras defect can be almost entirely compensated for by other gene products.

Ral GEFs, effectors of Ras-family GTPases, are activators of the two Ral proteins, RalA and RalB, which are also Ras-family GTPases (Wolthuis and Bos, 1999; Quilliam *et al.*, 2002; Rodriguez-Viciana *et al.*, 2004). It has been suggested that this Ral GEFs-Ral pathway is more important in the Ras-dependent oncogenesis of human cells than are other Ras-dependent pathways, such as those involving Raf and PI3K (Hamad *et al.*, 2002; Rangarajan *et al.*, 2004; Lim *et al.*, 2005; Gonzalez-Garcia *et al.*, 2005). The activated Ral then binds to various Ral-binding proteins and thereby regulates

This article was published online ahead of print in *MBC in Press* (http://www.molbiolcell.org/cgi/doi/10.1091/mbc.E06-08-0765) on March 7, 2007.

[D] [V] The online version of this article contains supplemental material at *MBC Online* (http://www.molbiolcell.org).

Address correspondence to: Michiyuki Matsuda (matsudam@path1.kyoto-u.ac.jp).

Abbreviations used: EGF, epidermal growth factor; FRET, fluorescence (Förster's) resonance energy transfer; GAP, GTPase-activating protein; GEF, guanine nucleotide exchange factor; NPY, neuropeptide Y; PI3K, p110α subunit of phosphoinositide-3-kinase.

various cellular functions (Feig, 2003). The characterization of such Ral effector proteins has suggested that Ral may be involved in vesicular trafficking. For example, the Ral-binding protein RalBP1 is thought to regulate endocytosis, suggesting the involvement of Ral in endocytosis (Nakashima *et al.*, 1999). Ral may also regulate exocytosis, because Ral binds to two components of the exocyst complex, Sec5 and Exo84 (Moskalenko *et al.*, 2002, 2003).

The exocyst complex was originally identified by genetic and biochemical studies as a cluster of molecules required for exocytosis in budding yeast, and it was later characterized in a wide range of eukaryotes. The exocyst complex consists of eight subunits: Sec3, Sec5, Sec6, Sec8, Sec10, Sec15, Exo70, and Exo84 (Lipschutz and Mostov, 2002). These proteins are primarily involved in the tethering and/or docking process of trafficking vesicles, which occurs before the fusion process (Finger *et al.*, 1998; Tsuboi *et al.*, 2005). Due to their fundamental role in exocytosis, any malfunction of the proteins in the exocyst complex can disrupt various cellular events, such as the basolateral transport of vesicles in polarized epithelial cells, neurite outgrowth in PC12 cells, paraxial mesoderm formation in mice, and secretory vesicle-mediated abscission in *Drosophila* (Friedrich *et al.*, 1997; Grindstaff *et al.*, 1998; Vega and Hsu, 2001; Murthy *et al.*, 2003; Gromley *et al.*, 2005).

To gain a better understanding of the function of R-Ras and its potential role in Ral-mediated exocytosis, it will be essential to elucidate not only the subcellular localization but also the activity change of these proteins. Thus, we developed specific anti-R-Ras sera and a probe for R-Ras activity based on the principle of fluorescence resonance energy transfer (FRET), a technique that has been shown to be extremely useful for the spatiotemporal analysis of small GTPases (Kurokawa *et al.*, 2004b). Using these tools, we found that endogenous R-Ras is enriched and activated at endosomes and that these R-Ras proteins promote exocytosis by activating RalA.

## MATERIALS AND METHODS

### *Probes Based on FRET*

FRET probes for R-Ras, designated as Raichu-R-Ras, were prepared essentially as described previously (Mochizuki *et al.*, 2001; Takaya *et al.*, 2004). From the amino terminus, Raichu-R-Ras consisted of a modified yellow fluorescent protein (YFP) designated as "Venus" (Nagai *et al.*, 2002) (amino acids [aa] 1-239), a spacer (Leu-Asp), human R-Ras (aa 1-199), a 17-amino acid-spacer (Gly-Gly-Gly-Thr-Gly-Gly-Gly-Gly-Gly-Ser-Gly-Gly-Thr-Gly-Gly-Gly-Thr), the Ras-binding domain of RalGDS (aa 785-871), a spacer (Gly-Gly-Arg), a modified cyan fluorescent protein (CFP) designated as "SECFP" ($Lys^{27}$Arg, $Asp^{130}$Ala, $Asn^{165}$His, $Ser^{176}$Gly) (aa 1-237), a spacer (Gly-Arg-Ser-Arg), and the carboxy-terminal region of R-Ras (aa 195-218) (Figure 1A). The characterization of Raichu R-Ras was performed as described previously (Takaya *et al.*, 2004).

### *Plasmids*

pCXN2-mCFP, pCXN2-mRFP, and pCXN2-mCherry are expression vectors encoding a monomeric SECFP (Zacharias *et al.*, 2002), a monomeric red fluorescent protein (RFP) (Kurokawa *et al.*, 2004a), and mCherry, respectively. cDNA of mCherry was provided by R. Y. Tsien (University of California at San Diego). The pERedNLS and pERedMito expression vectors contain an internal ribosomal site followed by the cDNAs of DsRed-Express (Clontech, Mountain View, CA) with nuclear and mitochondrial localization signals, respectively (Aoki *et al.*, 2005). pCXN2-5Myc and pCXN2-Flag are mammalian expression vectors containing Myc and Flag epitope tags, respectively. cDNAs of RalBP1 and Rgl were provided by A. Kikuchi (Hiroshima University, Hiroshima, Japan). cDNA of p110$\alpha$ and p85$\alpha$ were obtained from Y. Fukui (University of Tokyo, Tokyo, Japan), and cDNA of Rab5A was obtained from Y. Takai (Osaka University, Osaka, Japan). Rap1B cDNA was provided by N. Minato (Kyoto University, Kyoto, Japan). The cDNAs of K-Ras and N-Ras were obtained from L. A. Feig (Tufts University, Boston, MA). cDNAs of Rab7, Rab11A, and RalB were purchased from Guthrie cDNA Resource Center (Sayre, PA). pAcGFP1-Endo was purchased from Clontech. pVenus-N1-NPY was obtained from A. Miyawaki (The Brain Science Institute, RIKEN, Wako-shi, Japan) (Nagai *et al.*, 2002). pHA-EYFP-GH1 has been described previously (Matsuno *et al.*, 2005). pCXN2-Flag-CalDAG-GEFII, pCXN2-Flag-CalDAG-GEFIII, pCXN2-Flag-R-RasGAP, pCAGGS-Flag-p120RasGAP, pCXN2-Flag-rap1GAP1B, pCAGGS-RasGRF, pCAGGS-mSos1, and pEF-BOS-myc-Gap1$^{m}$ have been described previously (Yamamoto *et al.*, 1995; Gotoh *et al.*, 1997; Ohba *et al.*, 2000). pCXN2-5Myc-R-Ras-rRNAi (RNA interference-resistant clone) encodes a R-Ras mutant resistant to the short hairpin RNA (shRNA) vector. For the preparation of the glutathione S-transferase (GST) fusion proteins, cDNAs were subcloned into pGEX vectors and recombinant proteins were prepared according to the manufacturer's protocol (GE Healthcare, Little Chalfont, Buckinghamshire, United Kingdom).

### *Cells, Antibodies, and Reagents*

293T cells were obtained from B. J. Mayer (University of Connecticut, Storrs, CT). The line of Cos7 cells used in this study was Cos7/E3, a subclone of Cos7 cells established by Y. Fukui. The PC12 cells were obtained from S. Kuroda (University of Tokyo). HeLa and Madin-Darby canine kidney (MDCK) cells were purchased from the Human Science Research Resources Bank (Sennan-shi, Osaka, Japan). The GH3 cells used here have been described previously (Matsuno *et al.*, 2005). The PC12 cells were maintained in DMEM (Sigma-Aldrich, St. Louis, MO) supplemented with 10% fetal calf serum and 5% horse serum. GH3 cells were cultured in Ham's F-10 (Sigma-Aldrich) supplemented with 15% horse serum and 2.5% fetal calf serum. Other cells were maintained in DMEM supplemented with 10% fetal calf serum. GH3 cells stably expressing R-Ras were prepared essentially as described previously (Akagi *et al.*, 2003). Anti-green fluorescent protein (GFP) rabbit serum was prepared in our laboratory. Anti-RalA and anti-RalB were purchased from BD Biosciences (San Jose, CA). Anti-FLAG M2 and tetradecanoyl phorbol-13-acetate (TPA) was purchased from Sigma-Aldrich. Anti-Myc 9E10 was obtained from Santa Cruz Biotechnology (Santa Cruz, CA). Anti-GFP antibody was also purchased from Takara Bio (Otsu, Japan). Anti-Akt, anti-phospho Akt (Thr308), anti-phospho-mitogen–activated protein kinase kinase (MEK) 1/2 (Ser217/221), and anti-R-Ras were purchased from Cell Signaling Technology (Beverly, MA). Alexa 488 anti-rabbit immunoglobulin G (IgG), Alexa 488 anti-rat IgG, and Alexa 568 anti-mouse IgG were purchased from Invitrogen (San Diego, CA). To generate anti-R-Ras sera, three rabbits were injected with GST-R-Ras.

### *RNA Interference*

Synthetic siRNAs against R-Ras and Ral proteins were prepared as described previously (Oinuma *et al.*, 2004; Wozniak *et al.*, 2005). siRNAs were transfected using Oligofectamine or Lipofectamine 2000 (Invitrogen) according to the manufacturer's instructions. pSuper.retro.puro vector (OligoEngine, Seattle, WA) was used for short hairpin RNA. The shRNA sequences for rat R-Ras and RalA have been described previously (Oinuma *et al.*, 2004; Vitale *et al.*, 2005), and the sequence for rat RalB was 5′-GCCGACAGTTACAGAAAGA-3′. After transfection, the cells were incubated for at least 48 h before analysis.

### *Bos' Pull-Down Assay*

Bos' pull-down assay for Ral proteins was performed essentially as described previously (Takaya *et al.*, 2004). Briefly, the cells were lysed in Ral buffer (50 mM Tris-HCl, pH 7.5, 200 mM NaCl, 2.5 mM $MgCl_2$, 1% NP-40, 10% glycerol, 1 mM $Na_3VO_4$, 1 mM phenylmethylsulfunyl fluoride, 10 $\mu$g/ml aprotinin, and 10 $\mu$g/ml leupeptin) and were clarified by centrifugation. The supernatant was incubated with GST-Sec5-RBD or GST-RalBP1-RBD for 30 min at 4°C. The resulting complexes of Ral-GTP and GST fusion proteins were incubated with glutathione-Sepharose beads (GE Healthcare) for 1 h at 4°C, and after the bound proteins and cell lysates had been separated by SDS-polyacrylamide gel electrophoresis (PAGE), immunoblotting with anti-RalA or anti-RalB antibody was carried out. Bound antibodies were detected by an ECL chemiluminescence detection system (GE Healthcare), and binding was quantified with the aid of an LAS-1000 image analyzer (Fuji-Film, Tokyo, Japan). The pull-down assay for Ras, Rap1, and R-Ras was performed essentially as described above except for the use of GST-RalGDS-RBD.

### *Immunoprecipitation*

Transfected Cos7 cells were harvested in ice-cold lysis buffer (50 mM Tris-HCl pH 7.5, 200 mM NaCl, 2.5 mM $MgCl_2$, 1% NP-40, 0.5% sodium deoxycholate, 10% glycerol, 1 mM $Na_3VO_4$, 1 mM phenylmethylsulfunyl fluoride, 10 $\mu$g/ml aprotinin, and 10 $\mu$g/ml leupeptin). Anti-Myc antibody, GFP antiserum, or R-Ras antiserum was added to the cleared lysates. After the lysates were subjected to 1 h of rotation at 4°C with protein G-Sepharose or protein A-Sepharose (GE Healthcare), the beads were washed and boiled in sample buffer. The bound proteins were then subjected to immunoblot analysis.

### *Immunohistochemistry and Immunogold Electron Microscopy*

Formalin-fixed, paraffin-embedded sections were deparaffinized with xylenes and rehydrated with ethanol. The sections were treated with normal goat serum and 1% $H_2O_2$ to quench endogenous peroxidase activity, and then they

were incubated with primary antibody overnight at 4°C. After incubation of the sections with the biotinylated secondary antibody, immunopositive signals were visualized using 3,3'-diaminobenzidine tetrahydrochloride as a chromogen. For immunogold electron microscopy, the cells were fixed with 4% paraformaldehyde, 0.35% glutaraldehyde, and 0.2% picric acid at 4°C for 1.5 h, followed by fixation with 4% paraformaldehyde and 0.2% picric acid overnight at 4°C. After being washed with phosphate-buffered saline (PBS), the cells were dehydrated with ethanol and embedded in Lowicryl K4M (Polysciences; Tokyo, Japan). Ultrathin sections were placed on nickel grids and were immersed in a target retrieval solution (Dako Denmark, Glostrup, Denmark). Then, the samples were exposed to microwave radiation for 20 min, after which they were washed with distilled water. The grids were incubated with anti-R-Ras or preimmune rabbit serum at room temperature for 2 h, and then they were incubated for 1 h with anti-rabbit IgG labeled with 10-nm gold particles (GE Healthcare). After being washed and dried, the sections were stained with both uranyl acetate and lead citrate; the sections were then examined with a Hitachi H-800 transmission electron microscope (Hitachi High-Technologies, Tokyo, Japan). In some experiments, MDCK cells expressing an endosomal marker protein, AcGFP-Endo, were used for the analysis. Cells were double stained with anti-R-Ras rabbit serum and anti-GFP mouse monoclonal antibody (mAb) JL-8, which were detected with anti-rabbit IgG labeled with 5-nm gold particles and anti-mouse IgG labeled with 10-nm gold particles, respectively. As a control, anti-R-Ras rabbit serum preadsorbed to GST-R-Ras, preimmune rabbit serum, nonspecific rabbit IgG, or nonspecific mouse IgG was also used.

### *Immunocytochemistry*

To stain the endogenous R-Ras protein, MDCK cells were fixed with 3.7% formaldehyde and then subjected to refixation with methanol at −20°C and permeabilization with 0.2% Triton X-100, followed by incubation in PBS containing 3% bovine serum albumin (BSA) and 0.02% Triton X-100 for 1 h. In some experiments, MDCK cells were fixed with 4% paraformaldehyde, immediately followed by permeabilization with 0.01% Triton X-100 for 1 min and incubation with 2% BSA in 50 mM $NH_4Cl$-containing PBS. These fixed cells were incubated for 1 h at room temperature with anti R-Ras rabbit serum, washed with PBS, and then incubated for 30 min at room temperature with Alexa 488 anti-rabbit IgG. For the 3HA-tag and 5Myc-tag staining, Cos7 cells were fixed with 3% paraformaldehyde and subjected to permeabilization and staining as described above. Alexa 488 anti-rat IgG and Alexa 568 anti-mouse IgG were used to detect anti-hemagglutinin (HA) and anti-Myc, respectively. After being washed, the cells were imaged with an FV-500 confocal microscope equipped with an argon laser and with an HeNe laser microscope (Olympus, Tokyo, Japan). Twenty-five XY images scanned from the bottom to the top of the cells were obtained to prepare stacked images of XY and XZ sections.

### *Imaging of R-Ras and RalA Activity in Living Cells*

R-Ras and RalA activity was visualized with Raichu-R-Ras or Raichu-RalA essentially as described previously (Mochizuki *et al.*, 2001; Takaya *et al.*, 2004). Expression plasmids were transfected into Cos7 cells by Polyfect (QIAGEN, Valencia, CA) or 293fectin (Invitrogen). More than 36 h after transfection, the cells were imaged with an Olympus IX70 inverted microscope equipped with an image splitter, Dual-View (Optical Insights, Santa Fe, NM) and an EMCCD camera, iXon DV887 (Andor Technology, Belfast, United Kingdom), and the imaging process was controlled by MetaMorph software (Molecular Devices, Sunnyvale, CA). In some experiments, cells were imaged with an Olympus IX81 inverted microscope equipped with a laser-based autofocusing system, IX2-ZDC, and an automatically programmable XY stage, MD-XY30100T-Meta, which allowed us to obtain the time-lapse images of several view fields in a single experiment. For dual-emission ratio imaging of the Raichu probes, we used previously described filter sets (Takaya *et al.*, 2004), and we obtained images for CFP and FRET. After background subtraction was carried out, the FRET/CFP ratio was depicted using MetaMorph software, and this image was used to represent FRET efficiency. Confocal FRET images were obtained by an IX51 upright fluorescence microscope (Olympus) equipped with a CSU-10 spinning Nipkow disk confocal unit (Yokogawa, Tokyo, Japan), a W-view (Hamamatsu Photonics, Hamamatsu, Japan), and a diode-pumped solid state 430-nm laser (Melles Griot, Carlsbad, CA).

### *Exocytosis Assay*

The exocytosis assay was carried out using Venus-tagged neuropeptide Y (NPY) as described previously (Nagai *et al.*, 2002). pVenus-N1-NPY or pHA-EYFP-GH1 with or without additional expression vectors was transfected into PC12 cells or GH3 cells with Lipofectamine 2000 (Invitrogen). Sixty hours after transfection, the cells were washed in a low-potassium saline solution (145 mM NaCl, 5.6 mM KCl, 2.2 mM $CaCl_2$, 0.5 mM $MgCl_2$, 5.6 mM glucose, and 15 mM HEPES, pH 7.4). Then, the medium was exchanged for a high-potassium saline medium (95 mM NaCl, 56 mM KCl, 2.2 mM $CaCl_2$, 0.5 mM $MgCl_2$, 5.6 mM glucose, and 15 mM HEPES, pH 7.4) to depolarize the cells. After 20 min in the case of the PC12 cells or 10 min in the case of the GH3 cells, cell-free supernatants were collected and were stored as the secreted fraction. Cells remaining on the culture dishes were lysed in PBS containing 1% Triton X-100, and they were cleared by centrifugation to obtain the nonsecreted fraction. The fluorescence of NPY-Venus or EYFP-GH recovered in each fraction was measured by a FluoroSkan II fluorescence microplate reader (Global Medical Instrumentation, Ramsey, MN).

### *Online Supplemental Material*

Time-lapse FRET images of Supplemental Figure S3J and Figure 3B are compiled into QuickTime videos available as supplemental material. Movie 1 shows Cos7 cells transfected with pRaichu-R-Ras and stimulated with TPA as described in the legend to Supplemental Figure S3K. Movie 2 shows Cos7 cells transfected with pRaichu-R-Ras as described in the legend to Figure 2B. Images were acquired every 30 s, and the video is displayed at 15 frames per second. Supplemental Figures 1–6 show characterization of anti-R-Ras serum, images of colocalization studies, basic property of Raichu-R-Ras probe, and results of coimmunoprecipitation studies.

## RESULTS

### *Tissue Distribution of Endogenous R-Ras*

One of the reasons why the biological function of R-Ras remains elusive may be the lack of information concerning its tissue distribution and subcellular localization, which in turn is likely due to the lack of a specific antiserum. Therefore, we developed high-affinity anti-R-Ras sera that could be used for immunohistochemistry. One of the antisera was found to specifically recognize the endogenous R-Ras protein by immunoblotting analysis (Supplemental Figure S1). The obtained anti-R-Ras serum was used for immunohistochemical analyses. We found that R-Ras accumulated at high levels in the cytoplasm of smooth muscle cells, including those in the intestine and blood vessels, as has been reported recently (Komatsu and Ruoslahti, 2005) (Figure 1A). To a lesser extent, R-Ras expression was also observed in the neuroendocrine cells of the adrenal medulla and in islet cells in the pancreas (Figure 1B). Immunohistochemistry analysis in other tissues is described in Supplemental Figure S2.

### *Localization of Endogenous R-Ras on the Vesicular Structures Related to Early and Recycling Endosomes*

To more closely analyze the subcellular distribution of R-Ras, we chose MDCK cells, which were found to express R-Ras most abundantly among the cell lines examined (Supplemental Figure S1C). Quantitative immunoblotting analysis revealed that the number of R-Ras molecules was $1.5 \times 10^5$/cell, which was about one fifth of the number of Ras molecules but similar to the numbers of RalA and RalB molecules (data not shown). In MDCK cells, endogenous R-Ras was enriched on the vesicles and/or on endosome-like structures, although weak staining of the plasma membrane was also clearly seen (Figure 1, C and D). Such vesicular structures were not observed with preimmune sera or anti-R-Ras serum preabsorbed with antigen (data not shown). To further investigate the nature of R-Ras–positive endosomes, R-Ras was coexpressed with endosomal markers (Figure 2). R-Ras localization was found to overlap significantly with that of transferrin (early and recycling endosomes), Rab4A (early and recycling endosomes), Rab5A (early endosome), and Rab11A (recycling endosome), but not with that of EEA1 (early endosome) and Rab7 (late endosome). Immunoelectron micrographs showed that R-Ras was localized on cytoplasmic vesicular structures that were ~50 nm in diameter (Figure 1E). Furthermore, double staining showed the colocalization of R-Ras and AcGFP-Endo, an endosomal marker (Figure 1F). These results indicated that the R-Ras–loaded vesicles were related to early and recycling endosomes, but not to the late endosomes.

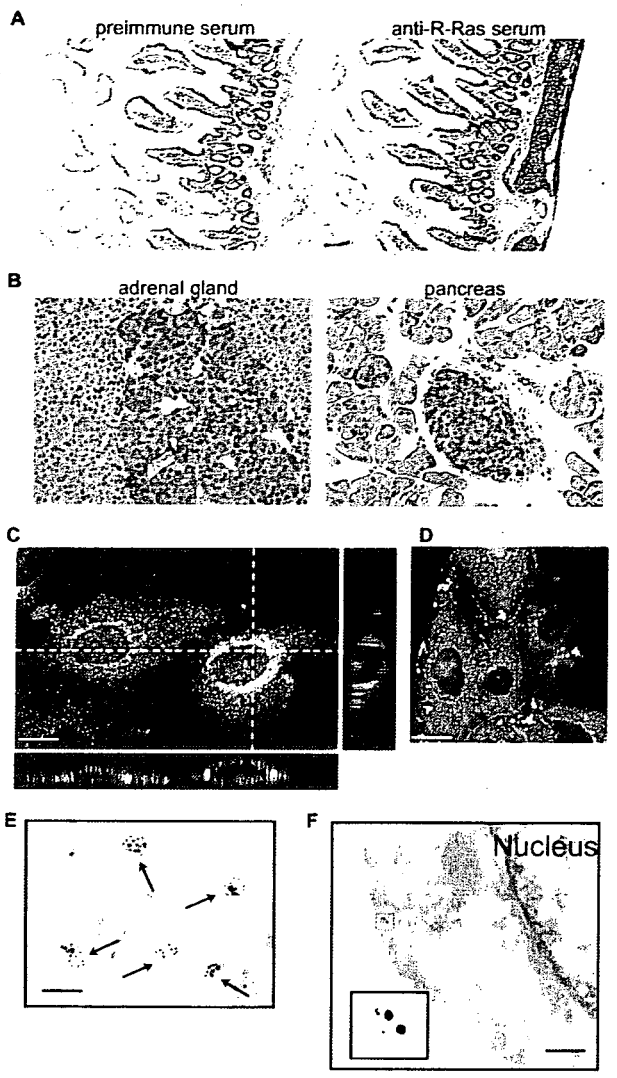


**Figure 1.** Tissue distribution and subcellular localization of R-Ras. (A) Immunohistochemistry analysis of mouse intestine with preimmune (left) or anti-R-Ras serum (right). Bound antibodies were detected with diaminobenzidine tetrahydrochloride, and the nuclei were counterstained with hematoxylin. Note the staining of the smooth muscle cell layer. (B) Immunohistochemistry of the mouse adrenal gland and pancreas. Note the staining of the adrenal medulla and Langerhans' islands. MDCK cells were fixed in 3.7% formaldehyde and methanol (C) or 4% paraformaldehyde (D) as described in the text, stained with the anti-R-Ras serum and the Alexa 488-coupled anti-rabbit IgG antibody, and observed with a confocal fluorescent microscope. Twenty-five XY images were obtained from the bottom to the top of the cells to prepare the stacked XY image. Cross sections are also shown at the dotted lines. Bar, 10 μm. (E) Immunoelectron micrograph of a MDCK cell stained with anti-R-Ras serum before detection with anti-rabbit IgG labeled with 10-nm gold particles. Bar, 100 nm. (F) Immunoelectron micrograph of a MDCK cell expressing an endosomal marker protein, AcGFP-Endo. Cells were double-stained with anti-R-Ras rabbit serum and anti-GFP mouse mAb JL-8, which were detected with anti-rabbit IgG labeled with 5-nm gold particles and anti-mouse IgG labeled with 10-nm gold particles, respectively. Inset depicts the magnified image of the gold particles. Bar, 100 nm.

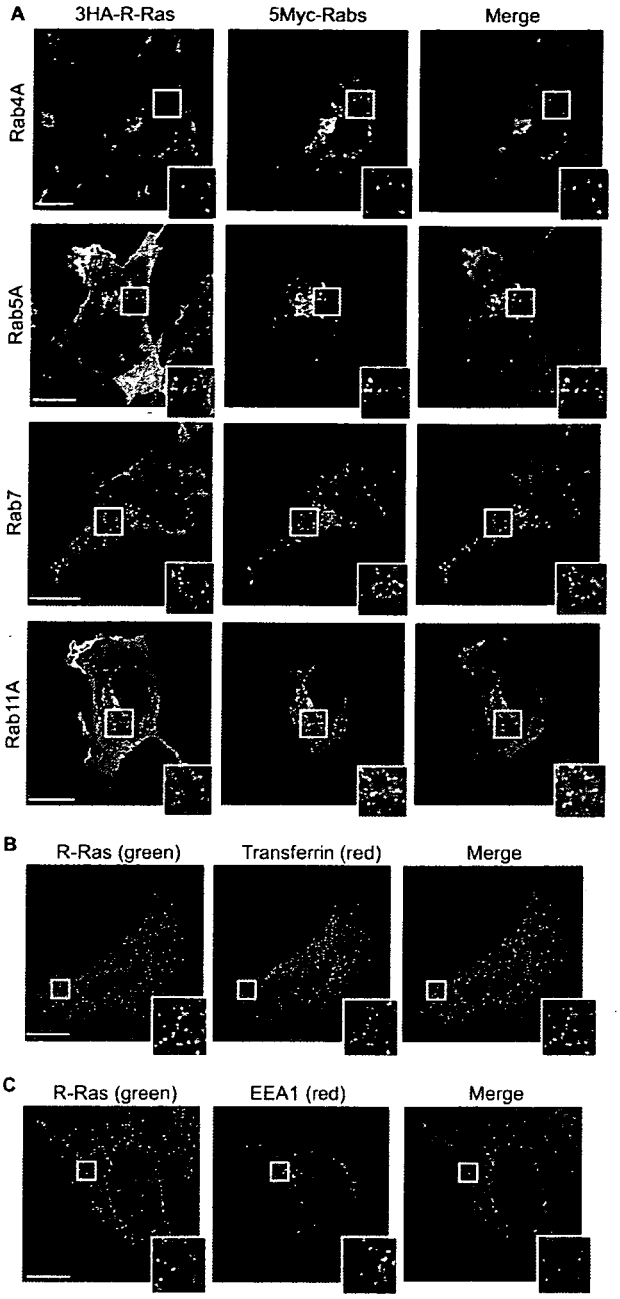


**Figure 2.** Colocalization of R-Ras with early and recycling endosome markers. (A) Cos7 cells expressing 3HA-tagged R-Ras and 5Myc-tagged Rab4A (early and recycling endosome marker), Rab5A (early endosome marker), Rab7 (late endosome marker), or Rab11A (recycling endosome marker) were double stained with anti-HA and anti-Myc antibodies and then observed with a laser-scanning confocal microscope. In the merged images, the red and green areas indicate anti-Myc and anti-HA antibodies, respectively. Bar, 10 μm. Outlined regions were enlarged and are shown in the insets. (B) Cos7 cells were incubated with Alexa-568-conjugated transferrin for 60 min and then stained with anti-R-Ras serum. (C) Cos7 cells were double stained with anti-R-Ras serum and anti-EEA1 antibody. Bar, 10 μm. Outlined regions were enlarged and are shown in the insets.

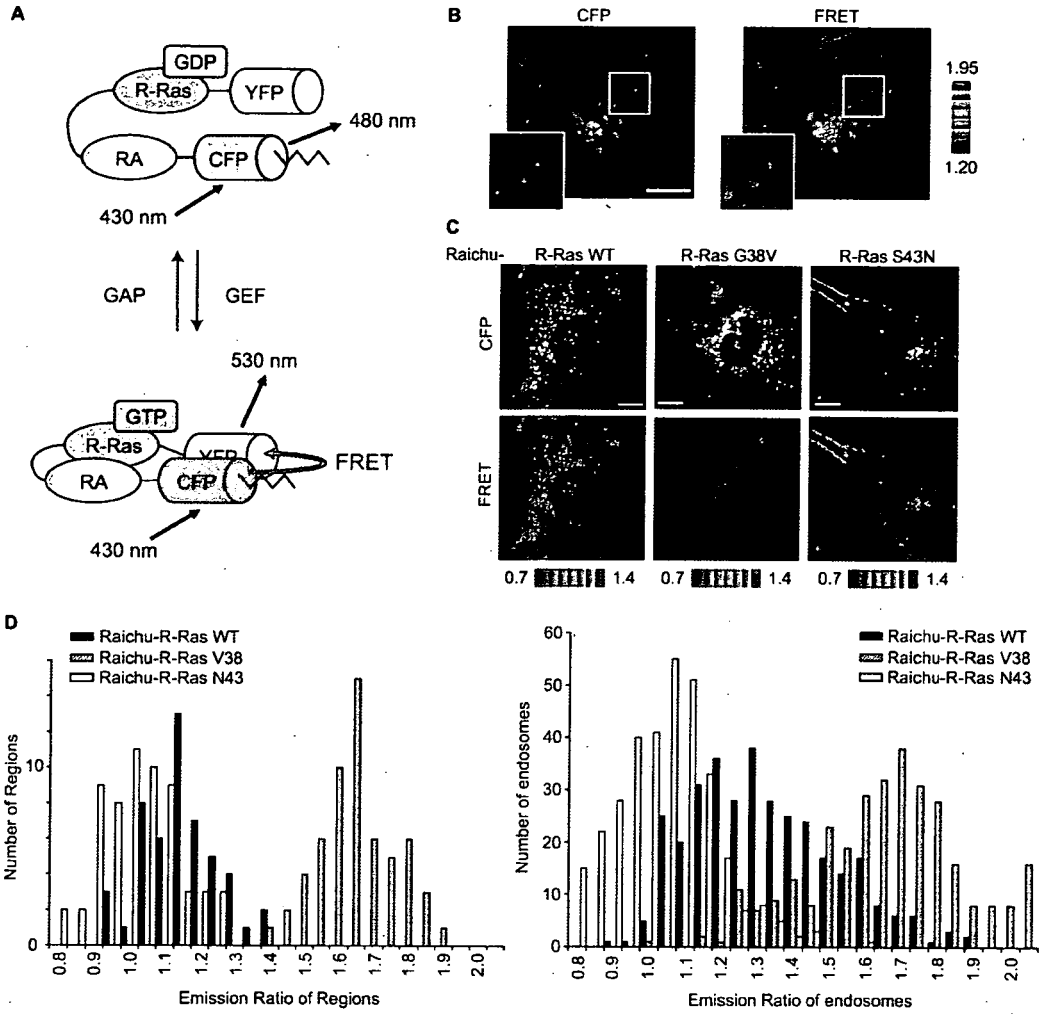


**Figure 3.** High R-Ras activity on the endosomes. (A) Schematic representation of the Raichu-R-Ras probe. Raichu-R-Ras consisted of a modified YFP designated as Venus, R-Ras, the RA domain (RA) of RalGDS, a modified CFP designated as SECFP, and the carboxy-terminal hypervariable region of R-Ras (indicated by the zigzag lines). On R-Ras activation, the intramolecular binding of R-Ras to the RA domain brings CFP into proximity with YFP, evoking YFP-derived fluorescence by the sensitized FRET. (B) A Cos7 cell expressing Raichu-R-Ras was imaged for CFP (excitation 430 nm/emission 480 nm) and YFP (excitation 430 nm/emission 530 nm). The images of the ratio (YFP versus CFP) were generated to represent the level of FRET. The upper and lower limits of the ratio range are shown on the right. Outlined regions are shown enlarged in the insets. Bar, 10 μm. (C) Cos7 cells expressing Raichu-R-Ras and its mutants were imaged with a confocal microscope. Bar, 10 μm. (D) FRET efficiency (YFP/CFP ratio) of Raichu-R-Ras, Raichu-R-Ras G38V, and Raichu-R-Ras S43N at the plasma membrane (left) and on the endosomes (right). For the endosomes, regions that exhibited higher CFP intensity than an appropriate threshold level were selected, and their YFP and CFP intensities were obtained. For the plasma membrane, three appropriate regions were arbitrarily selected, and the averages of their YFP and CFP intensities were obtained. Data from at least seven cells are shown in the histograms.

### *Development of a Probe for R-Ras, Raichu-R-Ras*

The unexpected observation that R-Ras was enriched on the endosomes urged us to investigate the role played by R-Ras on endosomes. For this purpose, we developed a series of FRET probes for the live-cell imaging of R-Ras activity. For the sake of brevity, only the results obtained with the Raichu-205X probe (hereafter referred to as "Raichu-R-Ras") are described here, because this probe performed best among those tested. From the amino terminus, Raichu-R-Ras includes a modified YFP designated as Venus, human R-Ras (aa 1-199), the Ras-association domain of RalGDS (aa 785-871), a modified CFP referred to as SECFP, and the carboxy-terminal hypervariable region of R-Ras (aa 195-218) (Figure 3A). Raichu-R-Ras fulfills most requirements for a FRET probe as described in the Supplemental Material and Supplemental Figure S3.

### *Activation of R-Ras on Endosomes*

Using Raichu-R-Ras, we visualized R-Ras activity in living Cos7 cells. The distribution of the Raichu-R-Ras probe was indistinguishable from that of the authentic R-Ras: The probe was enriched on the endosomes, but also localized diffusely on the plasma membrane (Figure 3B, Supplemental Figure S4, and Supplemental Movie 2). R-Ras activity, as visualized by the FRET level, was higher on the endosomes than on the plasma membrane. The high R-Ras activity observed on endosomes was more clearly observed with a